



UNIVERSITY OF LEEDS

This is a repository copy of *Where is my sink? Reconstruction of landscape development in 1 southwestern Africa since the Late Jurassic*.

White Rose Research Online URL for this paper:  
<http://eprints.whiterose.ac.uk/109731/>

Version: Accepted Version

---

**Article:**

Richardson, JC, Hodgson, DM [orcid.org/0000-0003-3711-635X](https://orcid.org/0000-0003-3711-635X), Paton, D et al. (3 more authors) (2017) *Where is my sink? Reconstruction of landscape development in 1 southwestern Africa since the Late Jurassic*. *Gondwana Research*, 45. pp. 43-64. ISSN 1342-937X

<https://doi.org/10.1016/j.gr.2017.01.004>

---

© 2017 International Association for Gondwana Research. Published by Elsevier B.V. This manuscript version is made available under the CC-BY-NC-ND 4.0 license  
<http://creativecommons.org/licenses/by-nc-nd/4.0/>

**Reuse**

Unless indicated otherwise, fulltext items are protected by copyright with all rights reserved. The copyright exception in section 29 of the Copyright, Designs and Patents Act 1988 allows the making of a single copy solely for the purpose of non-commercial research or private study within the limits of fair dealing. The publisher or other rights-holder may allow further reproduction and re-use of this version - refer to the White Rose Research Online record for this item. Where records identify the publisher as the copyright holder, users can verify any specific terms of use on the publisher's website.

**Takedown**

If you consider content in White Rose Research Online to be in breach of UK law, please notify us by emailing [eprints@whiterose.ac.uk](mailto:eprints@whiterose.ac.uk) including the URL of the record and the reason for the withdrawal request.



[eprints@whiterose.ac.uk](mailto:eprints@whiterose.ac.uk)  
<https://eprints.whiterose.ac.uk/>

1 Where is my sink? Reconstruction of landscape development in  
2 southwestern Africa since the Late Jurassic

3 Richardson, J.C.<sup>1\*</sup>, Hodgson, D.M.<sup>1</sup>, Paton, D.<sup>1</sup>, Craven, B.<sup>1</sup>, Rawcliffe, A.<sup>1</sup> and  
4 Lang, A.<sup>2</sup>

5

6 Affiliations

7 <sup>1</sup>School of Earth and Environment, University of Leeds, UK

8 <sup>2</sup>Department of Geography and Geology, Universität Salzburg, Austria

9 [\\*eejcr@leeds.ac.uk](mailto:eejcr@leeds.ac.uk)

10

11 **ABSTRACT**

12

13 Quantifying the rates and timing of landscape denudation provides a means to  
14 constrain sediment flux through time to offshore sedimentary basins. The Late  
15 Mesozoic evolution of drainage basins in southern Africa is poorly constrained  
16 despite the presence of several onshore and offshore sedimentary basins. A novel  
17 approach has been developed to calculate the volume of material eroded since the  
18 Late Jurassic at different time steps by constructing structural cross-sections and  
19 extrapolating thicknesses of eroded material. Using different assumptions, the  
20 calculated volumes of material eroded from southwestern Africa range from 2.52  
21  $\times 10^6$  km<sup>3</sup> (11.3 km of vertical thickness removed) to 8.87  $\times 10^5$  km<sup>3</sup> (4.0 km of vertical  
22 thickness removed). For the southward draining systems alone, the calculated  
23 removal of 7.81  $\times 10^5$  – 2.60  $\times 10^5$  km<sup>3</sup> of material is far greater than the volumes of  
24 sediment recorded in offshore sedimentary basins (268 500 km<sup>3</sup>). Reconstruction of  
25 the drainage systems using geomorphic indicators and clast provenance of the  
26 Uitenhage Group, as well as extrapolated surface exposure ages, indicate the

27 southern draining systems were active from the Late Jurassic with coeval activity in  
28 axial and transverse drainage systems. The calculated volumes are tied to published  
29 apatite fission track (AFT) dates to constrain the changes in exhumation rate through  
30 time (using multiple scenarios), which indicate a significant amount of Early  
31 Cretaceous exhumation (up to  $1.26 \times 10^6 \text{ km}^3$ , equivalent to 5.70km of vertical  
32 thickness). For the first time, this has permitted long-term landscape evolution to be  
33 used to support the interpretation that some of the 'missing' sediment was deposited  
34 in sedimentary basins on the Falkland Plateau as it moved past southern Africa  
35 during the Early Cretaceous. This implies that in this instance, the sinks are  
36 separated from their source areas by ~6000 km.

37

38 Key words: Drainage reconstruction, Mesozoic basins, Falklands Plateau basins,  
39 southern Africa, source-to-sink.

40

41 Highlights:

- 42 • The geomorphology of southern Africa is a record of Cretaceous drainage  
43 patterns
- 44 • The sink of eroded sediment is speculated to be the Falkland Plateau basins.
- 45 • The sink is separated by 6000km from its source.

46

## 47 **1. Introduction**

48

49 Reconstructing onshore routing patterns and landscape development is an  
50 important stage in the analysis of ancient source-to-sink configurations (e.g., Clift et  
51 al., 2006, Romans et al., 2009; Covault et al., 2011; Macgregor, 2012; Sømme and  
52 Jackson, 2013; Helland-Hansen et al., 2016). This relationship can be challenging to

53 constrain and quantify when assessing configurations in deep-time (i.e., Cretaceous  
54 and older) and close to active plate boundaries (Romans et al., 2009; Romans and  
55 Graham, 2013). Quantitative dating techniques such as in situ cosmogenic dating  
56 (e.g., Gosse and Phillips, 2001; von Blanckenburg and Willenbring, 2014), apatite  
57 fission track (AFT) (e.g., Gleadow et al., 1983, 1986; Gallagher et al., 1998), and (U-  
58 Th)/He thermochronology (Flowers and Schoene, 2010; Stanley et al., 2013) can  
59 place constraints on the timing and rate of erosion and exhumation. These  
60 approaches provide a means to understand onshore drainage basin configurations  
61 through time more accurately (e.g., Bierman, 1994; Gallagher and Brown, 1999;  
62 Cockburn et al., 2000) and when combined with remote sensing techniques, can aid  
63 offshore analysis by linking catchments areas to drainage evolution (McCauley et al.,  
64 1986; McHugh et al., 1988; Ramasamy et al., 1991; Blumberg et al., 2004; Gupta et  
65 al., 2004; Griffin, 2006; Youssef, 2009; Abdelkareem and El-Baz, 2015; Breeze et  
66 al., 2015).

67

68 South Africa is a passive margin (e.g., King, 1944; Fleming et al., 1999; Kounov et  
69 al., 2009), and comprises an interior plateau of low relief and high elevation,  
70 separated by the Great Escarpment from the coastal region of high relief and low  
71 average elevation. Large-scale river systems dominate the area to the north of the  
72 Great Escarpment such as the Orange River. Three large catchments control the  
73 area to the south of the escarpment: the Olifants, Breede and Gouritz catchments.  
74 The Great Escarpment forms the main drainage divide between the southward and  
75 westward draining systems.

76

77 Offshore southern South Africa there are several sedimentary basins (including the  
78 Bredasdorp, Pletmos (Infantaya Embayment), Gamtoos and Algoa basins) (McMillan  
79 et al., 1997). Despite the presence of these sedimentary basins, the onshore  
80 drainage development of river catchments south of the Great Escarpment has been  
81 under investigated (Rogers, 1903; Partridge and Maud, 1987). Landscape evolution  
82 research of South Africa has often focussed on the development and retreat of the  
83 Great Escarpment (e.g., King, 1953; Partridge and Maud, 1987; Fleming et al., 1999;  
84 Brown et al., 2002; Moore and Blenkinsop, 2006) and large-scale drainage systems  
85 such as the Orange River (e.g., Dingle and Hendry, 1984; Rust and Summerfield,  
86 1990; de Wit et al., 2000).

87

88 During the Cretaceous, there was large-scale exhumation of southern South Africa,  
89 recorded by AFT data (Brown et al., 1990; Tinker et al., 2008a). At the same time,  
90 large rift basins developed onshore and offshore during the fragmentation of  
91 Gondwana and opening of the southern Atlantic Ocean (Macdonald et al., 2003).  
92 Tinker et al. (2008a) reported 6.0 - 7.5 km of exhumation using AFT data, if the  
93 whole Karoo Supergroup succession was present, and identified two pulses of  
94 exhumation in the Early- and Mid-Late-Cretaceous, respectively. The Uitenhage  
95 Group represents the only onshore depositional representation of the Jurassic-  
96 Cretaceous exhumation event (Shone, 2006), although the age is contentious due to  
97 poor chronostratigraphic control, as discussed below. Previously, however, drainage  
98 reconstructions have not fully integrated information on the geomorphic evolution of  
99 the region or sedimentology of the Uitenhage Group to constrain the timing, routing,  
100 and volume of sediment flux from onshore drainage basins to offshore sedimentary  
101 basins.

102

103 This study aims to reconstruct the drainage history of two large drainage basins (the  
104 Gouritz and Breede catchments) in the Western Cape in order to: (1) calculate the  
105 maximum volume of material removed and compare relative timings with published  
106 AFT data; (2) compare the volume of material removed to the overall offshore  
107 sediment volumes during the Mesozoic; (3) examine the geomorphic indicators of  
108 river evolution and reconstruct the drainage evolution using geomorphological and  
109 sedimentological evidence, and (4) discuss where the 'missing' sediment was  
110 deposited during Mesozoic exhumation of southern South Africa.

111

## 112 **2. Regional setting**

113

### 114 2.1. Study area

115 The study area encompasses four onshore Mesozoic extensional basins in the  
116 Western Cape: the Oudtshoorn (study site - Kruisrivier Valley and N12), De Rust  
117 (study site - R341), Worcester (study site – Rooikrans) and Nuy (study site – Nuy  
118 Road) basins (Fig. 1). The onshore sedimentary basins are within two large  
119 discordant catchments in the Western Cape Province: the Gouritz (Richardson et al.,  
120 2016) and the Breede (Fig. 1), which have been developing since the Mesozoic  
121 break-up of Gondwana (Moore and Blenkinsop, 2002; Goudie, 2005; Hattingh,  
122 2008).

123

124 The Mesozoic sedimentary basins have been deeply exhumed and dissected (Fig. 1;  
125 Green et al., 2016). The Oudtshoorn Basin is bounded by the Kango fault and is the  
126 largest onshore Mesozoic basin with a length of 80 km across the E-W strike and a

127 width up to 21 km (Fig. 1). The Kango fault also bounds the De Rust Basin, which is  
128 37 km in length (E-W strike) and has a maximum width of 8 km. The Worcester and  
129 Nuy basins are bounded by the Worcester fault. The Worcester Basin is highly  
130 dissected and is approximately 27 km in length and 3 km in width; the Nuy Basin is  
131 15 km in length and 7 km in width. Hereafter, the Worcester and Nuy basins are  
132 referred to as the Worcester Basin.

133

## 134 2.2. Geology

135 The Cape and Karoo supergroups are extensively exposed in southern South Africa,  
136 with minor Pre-Cambrian metasediments (the Malmesbury, Kaaimans and Gamtoos  
137 groups) and granites (the Cape Granite suite) (Fig. 2). The Cape Supergroup is a  
138 siliciclastic succession composed of the Table Mountain, Bokkeveld and Witteberg  
139 groups (Broquet, 1992). The quartzitic Table Mountain Group represents shallow-  
140 marine sedimentation, with deposits including conglomerates, sandstones,  
141 mudstones, quartz arenites and mudstones. The argillaceous Bokkeveld Group  
142 represents deep-marine sedimentation. The Witteberg Group contains shallow  
143 marine quartzites and mudstones (Broquet, 1992). The Karoo Supergroup comprises  
144 the Dwyka, Ecca, Beaufort, Stormberg and Drakensberg groups. The Dwyka Group  
145 represents glacial sedimentation and comprises tillites. The Ecca and Beaufort  
146 groups contain claystone, siltstone, and sandstone. The deposits represent an  
147 overall shallowing-upward succession from basin-floor and submarine slope, through  
148 shelf, to fluvial and lacustrine depositional environments (Johnson et al., 1996; Flint  
149 et al., 2011). The Stormberg Group contains mudstones and sandstones, and  
150 represents sub-aerial and fluvial deposition (Johnson et al., 1996). The Drakensberg  
151 Group contains flood basalts and dolerites associated with the initial rifting of

152 Gondwana (Visser, 1984). The Uitenhage Group comprises deposits associated with  
153 the large-scale exhumation of southern South Africa during uplift and extension  
154 (Durrheim, 1987; Shone, 2006; Bordy and America, 2016), and contains the Enon,  
155 Kirkwood and Sunday River formations. The Enon and Kirkwood formations crop out  
156 in the study areas, and are remnants of once thicker and more laterally extensive  
157 extensional basin-fill successions (Fig. 1) (Shone, 1978). The Enon Formation is  
158 conglomeratic with silty/sandy matrix (Shone, 2006), which are intercalated with  
159 sandstone layers (McLachlan and McMillan, 1976), and has been interpreted as an  
160 alluvial fan deposit (Rigassi and Dixon, 1972; Hill, 1972; Winter, 1973). Deposition of  
161 the Enon Formation was coeval with rapid denudation as shown by the high  
162 sediment concentrations and boulder beds (Dingle, 1973; Lock et al., 1975). The  
163 Kirkwood Formation is variegated silty mudstone and sandstone, and represents a  
164 meandering fluvial environment (Shone, 2006).

165

166 Dating control within the Uitenhage Group is sparse. An unpublished radiometric age  
167 of 162 +/- 7 Ma for the underlying Suurberg Group, based on K-Ar whole-rock dating  
168 of a single basalt sample, represents a maximum age constraint for the Uitenhage  
169 Group (McLachlan and McMillan, 1976). However, due to erosion (e.g., Tinker et al.,  
170 2008a) and/or sediment bypass the depositional age may be much younger.

171 McLachlan and McMillan (1976) propose a Lower Valanginian to Berriasian age for  
172 the Enon and Kirkwood formations (~144-137 Ma); however, Green et al. (2016),  
173 assign a Tithonian to Valanginian age (151-136 Ma), based on data from Shone  
174 (2006) and Dingle et al. (1983). No onshore sediments of Jurassic age have been  
175 dated (McLachlan and McMillan, 1976). The Sunday River Formation, exposed in  
176 the Algoa Basin and onshore near the Coega River and Swartkops River Valley

177 contains ammonites, dated as Upper Valanginian to Hauterivian (~140-130 Ma)  
178 (McLachlan and McMillan, 1976). Nonetheless, Partridge and Maud (1987) assign a  
179 Late Jurassic age to Uitenhage Group conglomerates.

180

181 The offshore sedimentary basins (Fig. 1) are interpreted as extensional pull apart  
182 systems that formed during rifting of East and West Gondwana and the subsequent  
183 opening of the southern Atlantic (Brown, 1995; McMillan et al., 1997; Paton, 2006;  
184 Tinker et al., 2008b; Sonibare et al., 2015). The change from net deposition to net  
185 erosion in the Western Cape area is related to Gondwana rifting and lowered base  
186 levels of the continent at this time. This caused intense exhumation of the Karoo  
187 Basin-fill and the Cape Fold Belt (CFB), and the development of southward draining  
188 rivers (Gilchrist et al., 1994). Offshore deposition of conglomerates in the Uitenhage  
189 Group have been recorded in the major sedimentary basins of the inner Outeniqua  
190 Basin. The timing of initial deposition is diachronous across the offshore sedimentary  
191 basins (Dingle and Scrutton, 1974), which could relate to the time taken for transport  
192 offshore into the sedimentary basins or uncertainties in dating the offshore deposits.  
193 The first appearance of conglomerate offshore is Late Jurassic in the Bredasdorp  
194 Basin (Sonibare et al., 2015), Early Cretaceous in the Pletmos Basin (Brink et al.,  
195 1993), and Late Jurassic to Early Cretaceous in the Gamtoos Basin (Thomson,  
196 1999) and Algoa Basin (Dingle, 1973). The widespread presence of conglomerates  
197 offshore indicate that onshore erosion and sediment transport has been establish by  
198 the Late Jurassic and Early Cretaceous.

199

200 Tinker et al. (2008b) calculated an order of magnitude difference between the  
201 amount of sediment eroded onshore and the volume of sediment in the inner

202 Outeniqua Basin, the collective name for the Bredasdorp, Pletmos, Gamtoos and  
203 Algoa basins (Fig. 1), and outer (Southern) Outeniqua Basin. The volume of offshore  
204 sediment accumulation since ~136 Ma was estimated to account for 860 m of  
205 onshore exhumation, and a lag of 7 Ma was constrained from onshore denudation to  
206 offshore accumulation from 93 Ma to 67 Ma (Tinker et al., 2008b). Tinker et al.  
207 (2008b) calculated the variations in sediments volumes deposited in the offshore  
208 Outeniqua Basin, and reported episodes of increased sedimentation during ~136 –  
209 130 Ma ( $48,800 \times 10^4 \text{ km}^3$ ), 130 – 120 Ma ( $57,500 \times 10^4 \text{ km}^3$ ) and 93 - 67 Ma ( $83,700$   
210  $\times 10^4 \text{ km}^3$ ). During ~120 – 93 Ma, a volume of  $47,400 \times 10^4 \text{ km}^3$  was deposited, and  
211 decreased in the Cenozoic (67 – 0 Ma) to  $31,200 \times 10^4 \text{ km}^3$ .

212

213

### 214 2.3. Structure

215 Structurally, the Western Cape is dominated by the exhumed Cape Fold Belt (CFB),  
216 which is a compressional mountain range that formed in the late Permian and  
217 Triassic (e.g. Tankard et al., 2009; Flint et al., 2011). The CFB comprises resistant  
218 quartzite, as well as psammites and pelites, of the Cape Supergroup (Shone and  
219 Booth, 2005). Metamorphism within the Cape Supergroup reaches lowermost  
220 greenschist to anchizonal grade (Frimmel et al., 2001; Hansma et al., 2015).  
221 Greenschist facies form across a wide range of burial depth (8-50 km). However,  
222 considering the continental geothermal collision setting (between 25 and  $20^\circ\text{C km}^{-1}$ ;  
223 Frimmel et al., 2001), and assuming the density of overlying sediment of  $2.6 \text{ g cm}^{-3}$ ,  
224 12 – 15 km of overburden was estimated to reach  $300^\circ\text{C}$  (Frimmel et al., 2001 ).

225

226 Southern South Africa can be split into two broad tectonic domains defined as thick-  
227 and thin-skinned for the southern and northern domain, respectively (Paton et al.,  
228 2006). Uitenhage Group sediments accumulated in the hanging-wall of WNW-ESE  
229 trending half-graben basins formed by extensional faults during rifting (Paton, 2006).  
230 The faults are reactivated thrust faults that originally formed during the Late  
231 Palaeozoic/Early Mesozoic orogeny (Paton et al., 2006; Stankiewicz et al., 2007).  
232 The reactivated faults originated as long planes rather than individual segments,  
233 resulting in uplift across the entire planar surface (Paton, 2006). The Kango and  
234 Worcester faults show displacements of 6-10 km (Dingle et al., 1983; Tankard et al.,  
235 2009). The onshore basins (e.g., Oudtshoorn, Worcester, Heidelberg, Swellendam;  
236 Robertson) have not been assessed in detail (e.g., Söhnge, 1934; De Villiers et al.,  
237 1964; Du Preez, 1994; Lock et al., 1975), but contain Mesozoic sediment  
238 accumulation of up to 3000 m thickness (e.g., Oudtshoorn Basin).

239

#### 240 2.4. Geomorphology

241 Ancient landscapes (or 'Gondwanan landscapes'; Fairbridge, 1968) are a record of  
242 long-term and large-scale exhumation. The present-day river courses can be used to  
243 infer drainage evolution through superimposition and antecedence (e.g., Oberlander,  
244 1985; Summerfield, 1991; Stokes and Mathers, 2003; Stokes et al., 2008; Douglass  
245 et al., 2009). Certain landforms, such as deeply incised meanders in resistant  
246 lithologies or discordant drainage, are characteristic processes of superimposition or  
247 antecedence, as demonstrated in field and laboratory studies (e.g., Harvey and  
248 Wells, 1987; Douglass and Schmeckle, 2007). Superimposition is the process by  
249 which 'a river flowing over a young geological surface erodes the bedrock away and  
250 is lowered down onto an older more complex bedrock geology forming a drainage

251 which is transverse to the structure' (Stokes and Mather, 2003, page 61). Examples  
252 of superimposed rivers are known from many parts of the world including parts of the  
253 Himalayas (Summerfield, 1991); southern Spain (Harvey and Wells, 1987) and parts  
254 of the Colorado Plateau, America (Hunt, 1969). This process requires large-scale  
255 removal of rock in order to imprint a drainage pattern discordant to the underlying  
256 strata, ignoring the tectonic grain (Oberlander, 1985; Summerfield, 1991).

257

258 The geomorphology of the Eastern Cape and Northern Cape rivers has been used to  
259 interpret ancient major drainage reversals via stream capture events (de Wit et al.,  
260 2000; Hattingh, 2008). Major drainage reorganisation has occurred in the Orange  
261 River catchment (de Wit et al., 2000) due to continental uplift, as well as denudation  
262 onto the underlying structured pre-Karoo topography, which would also have  
263 affected catchments towards the south. Linking the landform record to the  
264 sedimentary record of the region has been rarely attempted. Drainage  
265 reconstructions based on sediments from the Uitenhage Group have argued for a  
266 connection between downdip basins, with lows in the surface topography of the CFB  
267 acting as sediment corridors (Lock et al., 1975). However, Rigassi and Dixon (1972),  
268 argued that the similarity between the onshore Mesozoic basins (Fig. 1) is due to the  
269 same type of depositional environment prevailing across southern South Africa. Also,  
270 Paton (2006) argued that the downdip basins of the Oudtshoorn area were  
271 separated by pre-rift strata. Rogers (1903) invoked a complicated drainage history of  
272 the Gouritz catchment whereby the Groot River captured the Buffels and Touws  
273 rivers (Fig. 3). Rogers (1903) also incorporated the Uitenhage Group deposits into  
274 the reconstruction, and argued that because there are no Uitenhage Group deposits  
275 in the transverse river valleys (e.g. Gamka River) they were not active at the time of

276 deposition. The reconstruction of the Gouritz drainage basin by Partridge and Maud  
277 (1987) has a planform similar to the present day, with extension of the tributaries to  
278 the north as the escarpment retreated. The lower portion of the catchment is also  
279 affected by changes in relative sea-level, with the river extending further onto the  
280 continental shelf in the mid-Cenozoic. Partridge and Maud (1987) integrated the  
281 presence of marine deposits and duricrusts into their reconstructions. Recently,  
282 Green et al. (2016) argued based on AFT data that the incision of the Gouritz  
283 Catchment into the Swartberg range is a Cenozoic event (30-20 Ma) that was driven  
284 by uplift.

285

286 Gilchrist et al. (1994) proposed that during Gondwana rifting, two drainage basin  
287 types developed in southern South Africa: internally draining catchments (e.g.,  
288 Kalahari and Karoo rivers) separated by the Great Escarpment from externally  
289 draining catchments, which formed as Gondwana rifted. The distance of retreat and  
290 formation of the escarpment are contentious. King (1966) argued the escarpment  
291 formed at the coastline and has since retreated to its current position. However,  
292 chronometric data and numerical modelling have concluded that the escarpment  
293 formed near its present-day position, with much of the retreat occurring in the  
294 Cretaceous and limited retreat thereafter (e.g., Fleming et al., 1999; van der Beek et  
295 al., 2002; Brown et al., 2002; Kounov et al., 2007). Published retreat rates and  
296 distances using AFT and cosmogenic data (Table 1), show that the escarpment has  
297 retreated a maximum of 29 km to its current-day position (Brown et al., 2002). In  
298 contrast, Green et al. (2016) use AFT from 7 samples in the Beaufort West area to  
299 argue that the Escarpment is the remnant of Cenozoic denudation (20-30 Ma) (Fig.  
300 3). There is variation in the retreat rate along the Great Escarpment, with higher

301 rates in the Drakensberg range where the escarpment is formed by basalt, and lower  
302 rates in Namibia, where the escarpment is formed on quartzites. The Drakensberg  
303 area also receives higher rainfall, which could also account for the higher rates  
304 (Tinker, 2005). The Gouritz drainage basin has been affected by the retreat of the  
305 escarpment (Fig. 3). AFT data shows that large-scale exhumation has occurred in  
306 southern South Africa and that a large amount of sediment is missing from onshore  
307 Mesozoic basin-fills. Using cored boreholes, Tinker et al. (2008a) conclude that 3.3 -  
308 2.5 km of exhumation took place in the Mid-Late Cretaceous of the eastern Southern  
309 Cape, diminishing to 2.5 – 2.0 km in the western Southern Cape and argued that a  
310 maximum of 7 km may have been eroded in the Early Cretaceous if erosion of the  
311 Karoo volcanics are taken into account. Wildman et al. (2015) argue for up to 6.3 km  
312 of exhumation in the Early Cretaceous, with an average of 4.3 km over the study  
313 area of the southwestern Cape of South Africa; up to 6.6 km during the Mid to Late  
314 Cretaceous (average of 4.5 km) and up to 2.4 km in the Late Cretaceous to Early  
315 Cenozoic. Wildman et al. (2016) argued for 1 - 2 km of material removed in the Early  
316 Cretaceous in the Western continental margin of southern South Africa, and one  
317 sample suggested up to 4 km of exhumation during this time period; up to 4 km in  
318 the Late Cretaceous and; up to 1 km in the Cenozoic, decreasing to 0.5 km from 30  
319 Ma. Green et al. (2016) argued for three phases of exhumation and sediment  
320 accumulation during the Cretaceous, with a regional cooling event in the Late  
321 Cretaceous (85-75 Ma). However, these authors did not attempt to estimate the  
322 volumes of material removed and the resulting lithological thickness were not  
323 calculated.

324

325 The mechanisms of the large-scale exhumation remain contentious (e.g. Doucouré  
326 and de Wit, 2003; de Wit, 2007; Paton, 2011), with Tinker et al. (2008a) noting that  
327 Early and Late Cretaceous exhumation are related to mantle activity and the  
328 formation of large igneous provinces and kimberlites. Wildman et al. (2015) argued  
329 for increased regional exhumation in the Early Cretaceous due to the rifting of  
330 Gondwana. Furthermore, elevation gain of 2 km (Cox, 1989) associated with plume  
331 activity could have provided the energy to drive the change from deposition to  
332 erosion (Cox, 1989; Nyblade and Sleep, 2003).

333

### 334 **3. Methodology**

#### 335 3.1. Volume of material removed

336 A grid of nine structural cross-sections (6 N-S and 3 E-W) were constructed across  
337 the Western Cape (study area of ~224, 200 km<sup>2</sup>) using 1:250 000 geological map  
338 sheets (Fig. 4; sheet numbers: 3218 Clanwilliam; 3220 Sutherland; 3222 Beaufort  
339 West; 3319 Worcester; 3320 Ladismith; 3322 Oudtshoorn and; 3420 Riversdale).  
340 Key lithostratigraphic units were then extrapolated across the sections using  
341 maximum and minimum stratigraphic thickness data recorded within the literature  
342 (Table 2). The arc method (Busk, 1929) was used, where lithostratigraphic thickness  
343 is maintained (Table 2). A 3D model was constructed of the key intervals across the  
344 study area (Fig. 4) using Midland Valley's 3DMove software. The volume of material  
345 removed was calculated (Fig. 5) by using the difference between a base horizon and  
346 the top horizon interpolated from the top of individual cross-sections. The base  
347 horizon is a combination of the digital elevation model (DEM) of the present-day  
348 topography and the average height of the study area where cross-sections are  
349 extended at the coast. To establish **maximum** and **minimum** volumes of material

350 removed a number of assumptions that relate to the original tectono-stratigraphic  
351 configuration of the area prior to exhumation are made:

352 1. The cross-sections were constructed with the Drakensberg volcanics, which  
353 currently do not crop out in the Western Cape, as either absent at the time  
354 (minimum) or extended into the study area at a similar thickness to their present-day  
355 occurrence in the east (maximum). Xenoliths in kimberlites have been used to  
356 reconstruct palaeo-geomorphological evolution in central South Africa, and it is  
357 argued that ~1500 m of the Drakensberg Group lithologies (mainly Lesotho  
358 Formation) were in the Kimberly area at the time of eruption (183 Ma) (Hanson et al.,  
359 2009). It is highly likely, therefore, that the Drakensberg volcanics extended across  
360 the entire Karoo Basin. Additionally, AFT work by Green et al. (2016) found a high  
361 chlorine content in the Uitenhage Group sandstones, indicative of volcanogenic  
362 sources, which could have been derived from the denudation of the Drakensberg  
363 volcanics.

364 2. Only lithologies older than Cretaceous are included in the cross-sections, as the  
365 main period of exhumation occurred during the Cretaceous (Tinker et al., 2008a).  
366 Although the Uitenhage Group deposits are locally thick, they are minor compared to  
367 the volume of material removed. For example, the volume of Cretaceous deposits in  
368 the Oudtshoorn Basin, assuming a maximum fill of 3000 m (McLachlan and  
369 McMillian, 1976), is 6900 km<sup>3</sup>. Calculations did not take into account sills and dykes  
370 associated with Karoo volcanics (Encarnación et al., 1996) that may have been  
371 eroded. This would represent a minor additional volume given the mapped  
372 distribution of these features within the drainage basins (Fig. 2).

373 3. The cross-sections were constructed either with all post-Carboniferous deposits  
374 (the Karoo Supergroup) onlapping against the folds of the CFB (minimum) or with all

375 the eroded lithostratigraphic units conformable and maintaining a constant thickness  
376 across the CFB to the present-day coastline (maximum), which assumes that all  
377 folding is post-depositional. There is no evidence beyond the present shoreline to  
378 constrain the upper lithological bounding surface.

379 4. Although removal of this sediment would have had an impact on lithospheric  
380 loading the isostatic effect is non-trivial to calculate as it will be a function of crustal  
381 architecture, nature of the removed sediment, elastic thickness of the lithosphere  
382 and thermal regime of the lithosphere and asthenosphere. It is, therefore, beyond the  
383 scope of this study to consider the isostasy and we only consider the geometric  
384 response.

385

386 To minimise uncertainties in volume calculation, multiple scenarios were developed.  
387 The extension at the coast scenario extends the onshore geology a maximum of 100  
388 km offshore, limited to the Falklands Agulhas transform fault and it is assumed that  
389 the lithostratigraphic groups extended farther at a similar elevation to that at the  
390 coast. This is because the variation in coastline extent is not fully constrained,  
391 although analysis of the offshore basins suggests that it was broadly similar to the  
392 current day coastline (e.g., Paton, 2002; MacDonald et al., 2003; Paton and  
393 Underhill, 2004). When the current coastline is used this varies the output by ~30%  
394 of the maximum assumption.

395

### 396 3.2. Sedimentary analyses

397 To assess provenance and sedimentary environments of the Oudtshoorn, De Rust  
398 and Worcester Basins, five representative sedimentary logs (cumulative thickness of

399 67.4m) and 950 clast measurements were collected to record clast lithology, size  
400 and roundness, and imbrication.

401

### 402 3.3. Drainage network analyses

403 River planform can be used to infer the evolutionary history of a catchment and  
404 provide important insights into the geological development of the region (Twidale,  
405 2004). Aster 30m DEM from NASA Reverb (2015) for southern South Africa was  
406 analysed using ArcGIS. Present-day river patterns and catchment areas were  
407 extracted using the hydrological toolbox using a conditional (con) value of 3000  
408 (representative of a contributing drainage area of 3.35 km<sup>2</sup>) showing both perennial  
409 and ephemeral rivers (Abdelkareem et al., 2012; Ghosh et al., 2015). Evidence of  
410 stream capture was identified to constrain drainage evolution (Summerfield, 1991).  
411 Sharp changes in channel direction (~90°) indicate capture sites, where the previous  
412 river course of a beheaded stream leaves a dry upstream reach and fluvial deposits  
413 in an abandoned river valley (wind gaps) (Summerfield, 1991). Stream reversal can  
414 be shown by barbed confluences, whereby the tributary joins the main river at an  
415 anomalous angle (Haworth and Ollier, 1992). Misfit streams are valleys that have  
416 anomalous cross-sectional areas compared to the streams that currently occupy  
417 them (Dury, 1960). Misfit streams can form by variation in discharge (Dury, 1960)  
418 caused by extrinsic factors such as climate change and tectonic activity, or intrinsic  
419 factors such as stream capture (Summerfield, 1991). In alluvial settings, identification  
420 of misfit streams uses the degree of meandering and the underlying floodplain  
421 deposits (Dury, 1960), however due to the lack of accommodation in bedrock  
422 settings this is not possible. To assess stream misfit in bedrock settings the minimum  
423 bulk catchment erosion was calculated using ArcGIS, whereby a horizontal 'cap' is

424 placed on the catchment to establish the volume of material removed from the  
425 catchment area. Catchment area correlates with rate of erosion established from  
426 cosmogenic nuclide concentrations (Bellin et al., 2014). Therefore minimum bulk  
427 catchment erosion is also expected to correlate with catchment area and provides a  
428 measure of stream misfit. If the catchment area is too small or large for the extracted  
429 volumes, the catchment may be misfit. Ten catchments from different tectonic and  
430 climatic settings from a range of locations (Table 3) were chosen and compared to  
431 catchments in the study location. The minimum bulk catchment erosion method  
432 represents an underestimate of material removed as the watershed and interfluvial  
433 areas have also been lowered due to erosion (Brocklehurst and Whipple, 2002;  
434 Bellin et al., 2014).

#### 435 3.4. Cosmogenic nuclide dating

436 Cosmogenic dating using in situ produced cosmogenic nuclides was used to  
437 constrain the exposure ages of surfaces including erosional strath terraces. The  
438 highest accessible erosion surface in Gamkaskloof (Fig. 6) was dated using in situ  
439  $^{10}\text{Be}$ . The sample was crushed and the 0.25 - 0.5 mm grain fraction extracted and  
440 treated using standard lab procedures (Von Blanckenburg et al., 1996, 2004). The  
441  $^{10}\text{Be}/^9\text{Be}$  ratios were measured in BeO targets with accelerator mass spectrometry at  
442 ETH Zürich (Kubik and Christl, 2010). The sample was normalised to the ETH in-  
443 house secondary standard S2007N, 0.162 g of  $^9\text{Be}$  carrier was added to the sample,  
444 and uncertainties were propagated from AMS counting statistics and the 38%  
445 uncertainty on the blank sample. Incision rates were calculated using CRONUS  
446 (Balco et al., 2008), which uses the known decay rates of  $^{10}\text{Be}$ , and integrates  
447 sample information such as elevation, latitude and longitude, shielding and sample  
448 density.

449

450 The age of the drainage systems in the Western Cape, including the deeply incised  
451 gorges, are poorly constrained (e.g., Rogers, 1903; Davis, 1906; Maske, 1957;  
452 Green et al., 2016), but can be used to improve understanding of temporal links  
453 between drainage basins and sedimentary basins. The sample used in this study  
454 was from the highest accessible surface within Gamkaskloof (Fig. 6), which is one of  
455 three breaches of the CFB within the Gouritz drainage basin, and marks where the  
456 Gamka River transverses the resistant quartzites of the Cape Supergroup (the  
457 confluence with the Dwyka River is 9 km upstream). The calculated incision rate was  
458 then used to extrapolate the time taken (exposure age) to incise from the highest  
459 elevation point of the Swartberg to the present day river. Cosmogenic dating can be  
460 used for the last  $10^6$  years when using  $^{10}\text{Be}$  (Darvill, 2013), and southern South  
461 Africa has been shown to be in long-term steady state whereby the cosmogenic  
462 nuclide results are similar to results from AFT for the Cenozoic (e.g., Bierman and  
463 Caffee, 2001; Codilean et al., 2008).

464

### 465 3.5. Scenarios of exhumation: timing and thickness of material removed

466

467 To estimate the amount of material eroded from southern South Africa, during  
468 different periods of exhumation (e.g., Tinker et al., 2008a,b; Wildman et al., 2015;  
469 Wildman et al., 2016), different scenarios, based on AFT data and offshore  
470 accumulation rates (Tinker et al., 2008a,b; Wildman et al., 2015; Wildman et al.,  
471 2016) were developed with the thickness of sediment removed calculated for the  
472 Early Cretaceous; Mid Cretaceous; Late Cretaceous; Late Cretaceous to Early  
473 Cenozoic; Early Cenozoic to Mid Cenozoic; and Late Cenozoic were recorded.

474 These periods were established using the time periods of proposed exhumation  
475 using AFT and offshore accumulation; there is some overlap between time periods  
476 (Table 4). The relative change in exhumation is the change in thickness of material  
477 removed during each time period, using the minimum and maximum exhumation  
478 from each scenario. This was then applied to the data extracted using the 3D Move  
479 model, with an emphasis on the maximum and median exhumation for the entire  
480 study area, and the maximum exhumation constrained to the southern draining  
481 catchments. This allows the maximum thickness of material removed for each of the  
482 different scenarios, and the relative change in exhumation from the Late Jurassic to  
483 Cenozoic, to be constrained.

#### 484 **4. Results**

##### 485 4.1. Amount of exhumation

486

487 Table 5 shows the volumes of material removed and the corresponding average  
488 lithological thickness, over the study area of the cross-sections of ~224 200km<sup>2</sup>  
489 calculated from a range of different scenarios using the uncertainties outlined above  
490 (section 3.1). An absolute maximum of 2.52 x 10<sup>6</sup> km<sup>3</sup> of material was removed from  
491 the Late Jurassic-Late Cretaceous and modelled timing is discussed below (Section  
492 5.3), which equates to an average of 11.3 km thickness of material removed across  
493 the study area. This is reasonable when considering the metamorphic grade of the  
494 Cape Supergroup (Frimmel et al., 2001). Using the minimum assumptions, a volume  
495 of 8.87 x10<sup>5</sup> km<sup>3</sup>, which equates to 4.0 km thickness of material removed in the study  
496 area. When constraining this to the southern draining catchments only, the value is  
497 reduced to 2.60 x10<sup>5</sup> km<sup>3</sup>, which equates to 1.2 km thickness of material removed.  
498 This is much lower than expected given the metamorphic grade of the Cape

499 Supergroup (Frimmel et al., 2001). The median (using the maximum and minimum  
500 scenario assumptions) value indicates up to 7.6 km thickness of material removed  
501 (equivalent volume of  $1.71 \times 10^6 \text{ km}^3$ ) when including the Drakensberg Group.  
502 Limiting the data to the southerly draining catchments, 2.3 km thickness of material  
503 has been removed with the Drakensberg Group present, or 2.1 km thickness ( $4.66$   
504  $\times 10^5 \text{ km}^3$ ) without the Drakensberg Group. The median value is reasonable when  
505 considering AFT data (e.g., Tinker et al., 2008a). The variation in lithological  
506 thickness removed is shown in Figure 5, with maximum thicknesses over the CFB  
507 and in western South Africa.

508

## 509 4.2. Sedimentology

510

### 511 4.2.1. Sedimentary facies

512 Sedimentary logs were collected from the Enon Conglomerate (Fig. 7), the oldest  
513 unit of the Uitenhage Group in the Oudtshoorn and De Rust basins adjacent to the  
514 Kango fault, and in the Worcester basin farther from the boundary fault (the  
515 Worcester fault). Facies one (F1) comprises poorly-sorted to rare normally-graded  
516 clast-supported conglomerate with coarse sand to gravel grade matrix in 1 - 5 m-  
517 thick beds with common erosional bases (Fig. 7). Individual clasts have deeply  
518 weathered crusts (Fig. 7). Clast imbrication in the Worcester Basin suggests a  
519 dominant southeastward palaeoflow (Fig. 8). Facies two (F2) comprises poorly-  
520 sorted lenticular conglomerate beds (up to 3 m) with a coarse sand matrix (Fig. 7).  
521 Facies three (F3) comprise structureless to weakly laminated lenticular coarse sand  
522 to gravel beds that range in thickness from 0.10 to 1.2 m. Locally, beds contain  
523 dispersed clasts (up to 10 cm; Fig. 7). Facies 4 (F4) comprises lenticular medium-

524 and coarse-grained sandstones with pebble stringers (Fig. 7). There is no distinct  
525 difference in roundness or clast size between the different conglomeratic facies;  
526 however there are differences between basin-fills (Table 6). Clasts sizes from the  
527 Oudtshoorn Basin show a wide spread about the a, b and c axes (Table 6). Clasts  
528 are dominantly sub-rounded to sub-angular in the Oudtshoorn Basin and  
529 dominantly sub-rounded and rounded in De Rust (Fig. 8). The Worcester Basin  
530 clasts are smaller than those in Oudtshoorn or De Rust. There is a larger spread of  
531 clast sizes within the Rooikrans study site compared to the Nuy Road study site as  
532 shown by the standard deviation values.

533

#### 534 4.2.2. Clast provenance

535 The clasts in the Oudtshoorn and De Rust basins are dominated by quartzites of the  
536 Cape Supergroup (Fig. 8). The clasts within the Worcester Basin (Fig. 8) are  
537 primarily sandstones, mudstones and diamictite (Karoo Supergroup), but no  
538 quartzite clasts are found. No volcanic or dolerite clasts are observed.

539

#### 540 4.2.3. Depositional environment

541 The bi-modal clast data (Fig. 8) at Oudtshoorn suggest deposition in alluvial fans  
542 with short transport distances from the source to the basin (Shone, 2006; Hattingh,  
543 2008; Bordy and America, 2016). Additionally, well-rounded quartzites with  
544 weathered surfaces, which represent reworked sediment were also observed. The  
545 De Rust (Fig. 8) deposit is more rounded than at Oudtshoorn, which suggests  
546 greater transport distance from the source area. The Worcester deposit (Fig. 8) is  
547 more fluvial in character, as shown by the higher proportion of rounded and

548 imbricated clasts and the dominance of graded and laminated sandstone/gravel  
549 beds and erosion surfaces (Rastall, 1911).

550

### 551 4.3. Geomorphological evidence

552

553 The Gouritz and Breede catchments are dominated by trunk rivers with courses that  
554 are discordant to the underlying tectonic fold structures and extensional faults  
555 (Rogers, 1903). The trunk rivers are ancient rivers (Cretaceous in origin and related  
556 to 'Gondwana landscapes'; Fairbridge, 1968; Rabassa, 2010), with their courses  
557 superimposed onto the underlying strata (Fig. 9), and meanders deeply incised into  
558 resistant quartzite of the Cape Supergroup. Furthermore, the rivers have anomalous  
559 bends (Fig. 9), with angles of up to 90°, and barbed confluences indicating flow  
560 reversal. Three large-scale misfit streams are identified in the Gouritz catchment  
561 (Fig. 9, 10). Two of the catchments (Figs. 9a, c) investigated here, have higher  
562 minimum bulk catchment eroded volumes than similar sized catchments, and some  
563 larger catchments (Table 3; Figs. 1, 10), from the global data set. The one exception  
564 is a catchment in Bolivia (Insel et al., 2010), where erosion rates are extremely high  
565 due to tectonic activity in the Andes. The catchment at Garcia Pass (Fig. 9, inset a)  
566 does not show an anomalous volume, however Rogers (1903) identified a wind gap  
567 at this location related to a previous Buffels River course. Our data indicate that the  
568 stream capture took place prior to the full exhumation of the Cape and Karoo  
569 Supergroups, and capture occurred before the underlying Table Mountain Group  
570 was exposed.

571

572 4.4. Cosmogenic dating

573

574 The strath terrace dated at Gamkaskloof (Swartberg Range), is at a height of 90 m  
575 above the current-day river, with incision rates based on cosmogenic nuclides of  
576  $1.22 \pm 0.02 \text{ m.Ma}^{-1}$  (Fig. 6). Assuming constant rates, incision from the strath height  
577 to the current river took  $\sim 70 \text{ Ma}$ . Extrapolating cosmogenic data back to the start of  
578 the Cenozoic provides a crude constraint, but due to the steady state of southern  
579 South Africa since the start of the Cenozoic is deemed reasonable. Using the  
580 maximum Cretaceous exhumation rates of  $175 \text{ m.Ma}^{-1}$  (Tinker et al., 2008a) incision  
581 of  $\sim 6 \text{ km}$  of material removed would have taken  $35 \text{ Myr}$ . However, Cenozoic rates of  
582 incision are lower (e.g., Fleming et al., 1999; Cockburn et al., 2000; Bierman and  
583 Caffee, 2001; van der Wateran and Dunai, 2001; Kounov et al., 2007; Codilean et  
584 al., 2008; Dirks et al., 2010; Decker et al., 2011; Erlanger et al., 2012; Chadwick et  
585 al., 2013; Decker et al., 2013; Scharf et al., 2013; Bierman et al., 2014; Kounov et  
586 al., 2015), up to  $15 \text{ m.Ma}^{-1}$ , which would have taken  $66 \text{ Myr}$  to incise the  $1 \text{ km}$  deep  
587 gorges in the Cape Fold Belt.

588

589 4.5. Scenarios of exhumation history

590

591 Table 7 shows four different scenarios related to the exhumation history of southern  
592 South Africa (Tinker et al., 2008a,b; Wildman et al., 2015, 2016). For the Early  
593 Cretaceous period, a minimum of 18% of the total exhumation could be represented  
594 in this time period (Scenario 1) to a maximum of 47% (Scenario 2); this relates to  
595 exhumation of  $2.07 \text{ km}$  and  $5.30 \text{ km}$  thickness of material removed for the maximum  
596 exhumation respectively (and between  $1.39 \text{ km}$  and  $2.94 \text{ km}$  for the median

597 exhumation). During the Mid Cretaceous, 20% (Scenario 1) to 40% (Scenario 3) of  
598 the total exhumation is represented, relating to 2.47 and 5.47 km thickness of  
599 material removed, respectively for the maximum exhumation (and between 1.66 km  
600 and 3.08 km for the median exhumation). Total exhumation percentage increases  
601 during the Late Cretaceous, from 17% (Scenario 1) to 50% (Scenario 2), related to  
602 1.95 km and 5.65 km thickness of material removed, respectively for the maximum  
603 scenario (and between 1.31 km and 3.13 km for the median exhumation). During the  
604 Late Cretaceous - Early Cenozoic, the maximum exhumation decreases, and 14 %  
605 (Scenario 3) to 31% (Scenario 1) of the exhumation is represented, relating to 1.66  
606 km and 3.51 km thickness of material removed, respectively to the maximum  
607 exhumation (and between 1.12 km and 2.36 for the median exhumation).

608 Exhumation rates decrease further in the Cenozoic.

609 Exhumation rates decrease further during the Early to Mid Cenozoic. During this  
610 time, exhumation represents 60% (Scenario 4) to 6% (Scenario 3) of the total  
611 exhumation, equating to a maximum thickness of 2.50 km and 0.69 km material  
612 removed, or a thickness between 1.60 km and 0.8 km for the median exhumation.

613 Scenario 4 indicates that in the Late Cenozoic, exhumation rates decrease further to  
614 11% of the total, representing 1.26 km thickness of material removed (and 0.84 km  
615 for the median exhumation). Scenario 4 uses data from the western margin of  
616 southern Africa, and will not be used further in this study, but highlights that the  
617 exhumation discussed in this paper was of continental scale.

618

## 619 **5. Discussion**

620

### 621 **5.1. Evolution of onshore sedimentary basins**

622

623 The infill stratigraphy of onshore half-graben sedimentary basins were more than 2  
624 km thick (Green et al., 2016, Fig. 11). The precise timing of different half-graben  
625 subsidence, and the number of infill and incision cycles, remains poorly constrained.  
626 The clast composition of the remnant fill can be used to place constraints on the  
627 different evolutionary histories in relation to exhumation of the Karoo and Cape  
628 supergroups, and potential source areas. Karoo Supergroup clasts dominate the  
629 Worcester Basin (Fig. 2). This suggests that at the time of deposition, the depth of  
630 exhumation of surrounding source areas had not reached the Witteberg Group  
631 quartzites, which would have produced larger and more resistant clasts than the  
632 Karoo Supergroup (Fig. 8). The present-day distribution of Karoo Supergroup  
633 outcrops supports the presence of a drainage basin further north (Fig. 2). Karoo  
634 Supergroup rocks are unconformably overlain by the Uitenhage Group  
635 conglomerates in the Worcester Basin, which indicates significant exhumation (upper  
636 Ecca and Beaufort formations) before accumulation during the formation of the  
637 Worcester Basin. The small clast size and clast roundness, and the large proportion  
638 of sand, suggests that the sediment was not locally derived, although the  
639 conglomerates unconformably overly the Karoo Supergroup indicating significant  
640 erosion prior to deposition. The absence of material in the Worcester Basin of local  
641 Cape Supergroup provenance could be due to non-exposure of the Cape  
642 Supergroup or erosion of the younger basin-fill (Green et al., 2016). No clasts of the  
643 Beaufort or Drakensburg groups are found within the conglomerate. This could be a  
644 function of shallow burial and weakly lithified material, which was easily broken down  
645 to sand grade material (Tinker, 2005; Hanson et al., 2009; Green et al., 2016).  
646 However, the absence of dolerite clasts may be used to place a northern limit on the  
647 source area (Fig. 2). The Oudtshoorn and De Rust basin clasts are primarily Table

648 Mountain Group quartzites, which crop out at the basin margins (Fig. 2), and indicate  
649 deeper exhumation at this location at the time of basin formation and filling  
650 compared to the Worcester Basin.

651

## 652 5.2. Drainage basin reconstruction

653

654 The rivers in southern South Africa have undergone significant re-organisation since  
655 the break-up of Gondwana (Partridge and Maud, 1987; De Wit et al., 2000; Goudie,  
656 2005), and this is the case for the Gouritz catchment. As Gondwana started to rift,  
657 reactivation of thrust faults as long extensional faults (Paton et al., 2006) led to the  
658 development of half-graben basins with sedimentation and the initiation of net  
659 southward draining river systems on the rift margin (Gilchrist et al., 1994). The small  
660 coastal draining rivers would have eroded headward, due to the reduction of base  
661 level at the newly formed coastline capturing internal draining catchments (Gilchrist  
662 et al., 1994) that eroded the youngest unlithified shallowly buried deposits. Prior to  
663 deep exhumation of the Karoo Basin and the Cape Fold Belt, the large southerly  
664 drainage systems have already been in place as shown by their superimposed  
665 planform into resistant quartzites (Rogers, 1903), bedrock meanders with high  
666 gradients in the trunk rivers (Richardson et al., 2016), and the deeply incised  
667 confluence of the Olifants and Gouritz rivers. Furthermore, the large trunk rivers do  
668 not follow the tectonic grain of southern South Africa or follow geological lines of  
669 weakness (Richardson et al., 2016), which supports superimposition. Additional  
670 support for the ancient origin of the trunk rivers comes from estimates using  
671 cosmogenic dating of terraces in Gamkaskloof, in which the rivers had incised to 90  
672 m above the present-day river by the end of the Cretaceous. Superimposition,

673 supported by AFT analysis (e.g., Tinker et al., 2008a), requires a vertical component  
674 of incision (Maw, 1866; Gilbert, 1877; Rogers, 1903; Partridge et al., 2010), and is  
675 unlikely to have been formed solely by headward erosion from the coast (e.g.,  
676 Gilchrist et al., 1994). The data in Section 4.4 are plausible especially when  
677 considering the missing Cape and Karoo sequence above the strath terrace is not  
678 included in the age estimate, further a sample located at the top of the CFB showed  
679 Cretaceous exhumation (Green et al., 2016). However, alternatively, it has been  
680 argued that the trunk rivers, such as the Gamka River, could have formed more  
681 recently (30 - 20 Ma) (Green et al., 2016), with ~1 km incision into the resistant Cape  
682 Supergroup (Swartberg Range). However, this rapid incision is not supported by the  
683 majority of published AFT and cosmogenic studies that show low denudation rates  
684 since the Cretaceous (e.g., Tinker et al., 2008a,b; Scharf et al., 2013; Kounov et al.,  
685 2015), or the timing of offshore sedimentation.

686

687 In the Late Jurassic – Early Cretaceous, the rivers meandered (as shown by the  
688 superimposed planform, Fig. 11) and incised into shallowly buried volcanic  
689 (westward equivalent of Drakensburg Group) and fluvial deposits of the upper  
690 Beaufort Group. During incision, and net southward drainage, the rivers encountered  
691 increasingly deeply buried and more resistant rocks (Tinker et al., 2008a). The  
692 precise relationship between incision, local uplift and subsidence patterns during  
693 fault reactivation, is largely speculative. Nonetheless, the superimposed river  
694 systems, the deposition of the Enon conglomerate, the published apatite fission track  
695 studies (Brown et al., 1990; Brown et al., 2002; Tinker et al., 2008a), and the  
696 offshore basin stratigraphy (Dingle, 1973; Brown, 1995; McMillan et al., 1997; Paton  
697 and Underhill, 2004; Tinker et al., 2008b; Sonibare et al., 2015) all indicate large

698 volumes of material eroded and transported offshore in the Early and Late  
699 Cretaceous (Section 5.3). Exhumation was by efficient and well-established fluvial  
700 networks that were established by the Early Cretaceous (Tables 4 and 7) following  
701 the break-up of Gondwana (Fig. 11).

702

703 The deposition of the Mesozoic conglomerate in onshore half-graben basins was  
704 coeval with the exhumation and incision of the Cape Supergroup in the Oudtshoorn  
705 Basin. In the case of the western Oudtshoorn Basin, this suggests that transverse  
706 and axial drainage systems, and large-scale erosion of the bedrock and sediment  
707 accumulation, was penecontemporaneous but <1 km apart. Coeval axial and  
708 transverse drainages are well documented in tectonically-active settings, with relief  
709 increasing due to tectonic activity related to the early stage of mountain growth and  
710 are features of many mountain ranges of the world (e.g., Davis, 1889; Oberlander,  
711 1985; Hovius, 1996; Ramsey et al., 2008; Babault et al., 2012; Grosjean et al.,  
712 2015). The interplay between axial and transverse rivers is not well-documented  
713 using deposits alone (Szwarc et al., 2015). Many facies models related to basins in  
714 continental rift settings emphasise a major component of axial deposition with minor  
715 footwall-draining transverse systems (e.g., Leeder and Gawthorpe, 1987; Schlische,  
716 1992). These models do not account for large cross-cutting transverse river systems  
717 (e.g., Gawthorpe and Leeder, 2000) that can be an important component of rift  
718 settings after headward erosion of transverse rivers and integration of the entire  
719 drainage net (axial and transverse systems) (e.g. Gilchrist et al., 1994). In the case  
720 of the Gouritz catchment, there was large-scale net deposition within the axial river  
721 system and net erosion within the large transverse river system during the  
722 Cretaceous due to the position of drainage networks with respect to areas of uplift

723 (erosion) and subsidence (deposition). We speculate that the integration of the  
724 drainage net occurred rapidly at this location. The lack of deposits in the transverse  
725 rivers is due to the low preservation potential within bedrock channels due to high  
726 stream power and the net erosional setting (Hancock et al., 1998). This leads to  
727 efficient bypass of sediment to the offshore basins and does not necessarily indicate  
728 that the transverse systems were inactive during the deposition of the Uitenhage  
729 Group as postulated by Rogers (1903) and Green et al., (2016).

730

731 During the Early Cretaceous, there were drainage divides within the Olifants River  
732 due to pre-rift strata (Paton, 2006). Stream captures and a large-scale misfit stream  
733 indicate that part of the river system drained through the Oudtshoorn Basin to the  
734 confluence with the Gamka River, and another part drained eastward and  
735 discharged into the Indian Ocean at Jeffreys Bay (Figs. 9, 10). Drainage divides  
736 were located in the Touws River area, with westward stream flow to the Worcester  
737 Basin (Breede River), and partly to the east into the Buffels River, as supported by  
738 the provenance of the Mesozoic conglomerates in the Worcester Basin (Fig. 8). The  
739 Buffels River drained south, and influenced the onshore Heidelberg Basin as a  
740 conduit for sediment, as shown by the wind gap at Garcia Pass (Rogers, 1903).

741

742 Apatite fission track work by Green et al. (2016) concluded that at least 1.5 km of  
743 deposits overlay the remnant Enon conglomerate outcrops in the Oudtshoorn Basin  
744 in the Late Cretaceous (Fig. 11). The Enon conglomerate and the overlying deposits  
745 could represent one phase of net deposition. However, Green et al. (2016) speculate  
746 the material could be detritus from the Congo Inlier (north of the Oudtshoorn Basin)  
747 or be related to post-Drakensberg volcanism as the apatites from the Uitenhage

748 Group show high chlorine content, which is related to a volcanic source. The  
749 deposition of this material may have diverted the Olifants River within the floodplain,  
750 or formed epigenetic gorges (e.g. Ouimet et al., 2008). However, exhumation of the  
751 Cape Supergroup, and the CFB as a geomorphic feature towards the south, would  
752 have limited the space into which the river could have migrated. The Gamka River  
753 was powerful and able to incise the resistant Cape Supergroup and most likely  
754 continued as a conduit for sediment bypass during this period of sedimentation in the  
755 Outdshoorn Basin. Green et al. (2016) suggests episodic block uplift which would not  
756 have changed the overall regional gradient of the Western Cape and the rivers would  
757 still drain southward. A record of episodic uplift is no longer evident in the current  
758 river morphometric indices (Richardson et al., 2016). At the time of block uplift,  
759 however, propagating knickpoints will have formed during river adjustment to new  
760 regional base levels (e.g., Seidl et al., 1994, 1997; Wohl et al., 1994; Weissel and  
761 Seidl 1998; Stock and Montgomery, 1999), with faster response times to larger  
762 tectonic perturbations (Whittaker and Boulton, 2012). In addition, due to the high  
763 erosive power of the rivers during this time and the presence of transverse drainage  
764 systems, it is likely the rivers managed to keep pace with uplift rather than be  
765 deflected by it (e.g., Stokes et al., 2008; Douglass et al., 2009). This is due to the  
766 large catchment areas of the transverse trunk rivers, resulting in high stream power  
767 and knickpoint development (e.g., Burbank et al., 1996; Bishop et al., 2005). During  
768 uplift, large trunk rivers will try to maintain their gradients, which can result in  
769 aggradation upstream of the uplift (Burbank et al., 1996). If aggradation keeps pace  
770 with, or exceeds, uplift then the river will remain discordant to the structure due to the  
771 maintenance of the long profile gradient and resulting impacts on stream power  
772 (Burbank et al., 1996, Humphrey and Konrad, 2000). There is no evidence of

773 upstream aggradation remaining within the catchment, due to the large-scale  
774 denudation of southern South Africa (Tinker et al., 2008a; Green et al., 2016). If uplift  
775 exceeds aggradation then the transverse rivers must erode the block. In this case,  
776 the resistance of the block becomes a dominant control on the development of  
777 discordant rivers (Burbank et al., 1996). The trunk rivers were capable of incising  
778 deeply into quartzite, which indicates the rivers were powerful and likely to have  
779 eroded more easily the younger less resistant stratigraphy above the Table Mountain  
780 Group (Fig. 2). The morphometric indices of the Gouritz catchment indicate that the  
781 smaller stream order catchments are structurally-controlled within the CFB with  
782 trellised stream patterns, whereas the trunk rivers simply dissect the fold belt, with  
783 straight long profiles sections seen within the CFB region (Richardson et al., 2016).

784

785 The Groot River is interpreted to have captured the Buffels and Touws rivers, as  
786 indicated by the right-angled confluence (Fig. 9) (Rogers, 1903). Stream captures  
787 may have also occurred within the Olifants River, most likely resulting in a large-  
788 scale misfit stream towards the east (Fig. 9). The climate of the Western Cape  
789 Province has not changed significantly since the Cretaceous (Bakker and Mercer,  
790 1986) and the area is now relatively stable tectonically compared to the Cretaceous  
791 as shown by the lack of scarps and reduction in sediment production (e.g., Tinker et  
792 al., 2008b; Bierman et al., 2014). Therefore, stream capture is the preferred  
793 mechanism to explain the misfit streams. Further development towards the north of  
794 the Gouritz catchment due to the retreat of the escarpment extended the catchment  
795 and caused capture of the Orange River catchment area. Stream capture of the Hex  
796 River by the Touws River (Gouritz catchment) has reduced the size of the Breede  
797 catchment since the Cretaceous.

798

799 5.3. Implications for timing of exhumation and volumes of material transported  
800 offshore

801

802 Many researchers argue on the basis of AFT that large-scale exhumation had  
803 finished by the end of the Cretaceous (Gilchrist et al., 1994; Gallagher and Brown,  
804 1999; Cockburn et al., 2000; Brown et al., 2002; Tinker et al., 2008a; Kounov et al.,  
805 2009; Flowers and Schoene, 2010), with minor changes to the present-day  
806 physiography (Partridge, 1998; Brown et al., 2000; Brown et al., 2002; Doucouré and  
807 de Wit 2003; de Wit 2007; Tinker et al., 2008a; Kounov et al., 2015). Additional  
808 evidence is shown by a reduction in offshore sediment volumes (Tinker et al., 2008b;  
809 Paton et al., 2008; Hirsch et al., 2010; Dalton et al., 2015; Sonibare et al., 2015), low  
810 Cenozoic cosmogenic erosion rates (e.g., Fleming et al., 1999; Cockburn et al.,  
811 2000; Bierman and Caffee, 2001; van der Wateran and Dunai, 2001; Kounov et al.,  
812 2007; Codilean et al., 2008; Dirks et al., 2010; Decker et al., 2011; Erlanger et al.,  
813 2012; Chadwick et al., 2013; Decker et al., 2013; Scharf et al., 2013; Bierman et al.,  
814 2014; Kounov et al., 2015) and differential erosion of kimberlite pipes (Hawthorne,  
815 1975; Gilchrist et al., 1994; de Wit, 1999). Locally, offshore sedimentation in the  
816 Cenozoic is significant, but is minor compared to Mesozoic deposition (e.g., Tinker et  
817 al., 2008b; Hirsch et al., 2010; Dalton et al., 2015; Sonibare et al., 2015). Further,  
818 modelling by Gilchrist et al. (1994) argued that much of the denudation, and  
819 establishment of the drainage net of southern South Africa, occurred before the  
820 Cenozoic.

821

822 A range of scenarios were assessed using maximum and median exhumation. The  
823 data shown in Table 7, for the Early Cretaceous, is based on a limited number of

824 samples, but does indicate a significant amount of exhumation in this period (up to  
825 47%, Scenario 2), which is argued to be regional by Wildman et al. (2015). Up to  
826 40% of the exhumation is accounted for in the Mid Cretaceous (Scenario 3), which  
827 increased to 50% (Scenario 2) in the Late Cretaceous. All scenarios show a  
828 decrease in exhumation during the Late Cretaceous to Early Cenozoic with up to  
829 31% of exhumation represented (Scenario 1). This decreased further in the Early to  
830 Mid Cenozoic, when up to 20% of exhumation is represented (Scenario 2). As stated  
831 above, the majority of researchers have argued for periods of increased exhumation  
832 in the Early Cretaceous and Mid-Late Cretaceous, with limited exhumation in the  
833 Cenozoic. The majority of studies present clusters of data around the Mid-Late  
834 Cretaceous (e.g., Flowers and Schoene, 2010) and a few boreholes show Early  
835 Cretaceous cooling, particularly south of the escarpment (e.g., Tinker et al., 2008a).  
836 This is because there has been greater exhumation south of the escarpment, and  
837 the Early Cretaceous signature has been removed due to erosion and sediment  
838 bypass (e.g., Tinker et al., 2008a and Wildman et al., 2016) and explains the lack of  
839 boreholes with Early Cretaceous exhumation.

840

841 Despite the evidence above, such a scenario has been disputed by Burke (1996)  
842 and Green et al. (2016) who argue for a younger age of landscape development.  
843 Burke (1996) argued the topography and Great Escarpment was formed due to uplift  
844 around 30 Ma ago, and related to the establishment of the African superswell under  
845 the African lithosphere. Robert and White (2010), Roberts et al. (2012), and Rudge  
846 et al. (2015) have also argued for a Cenozoic age of the landscape with Cenozoic  
847 uplift and development of rivers within southern South Africa. However, their simple  
848 1D inversion models do not preclude Late Mesozoic development of the discordant

849 trunk rivers, and may represent a second phase of landscape development. Green et  
850 al. (2016) argued for younger active landscape development based on AFT data,  
851 and argued that the deep bedrock gorges within the CFB were formed during the  
852 Cenozoic, when there was differential denudation with higher erosion within the  
853 Swartberg Mountain range (CFB) as shown by Cenozoic cooling (30-20 Ma).  
854 However, Green et al. (2016) did not collect samples near the large cross-cutting  
855 transverse rivers of the Gouritz catchment (e.g., Gouritz River), and were from  
856 smaller subcatchments that dissect the CFB (with current catchment areas of 179  
857 km<sup>2</sup> and 1060 km<sup>2</sup>). The samples showing Cenozoic cooling were taken at the base  
858 of the Swartberg Mountain, near the current river bed, and do not indicate that the  
859 large trunk rivers were not already active, and eroding the ~1 km of material above  
860 the sample. Green et al.'s (2016) research indicates that there was additional uplift  
861 around 30-20 Ma ago, during which downcutting would have continued in gorges  
862 existing at the time. The CFB is an exhumed mountain belt that formed during the  
863 Permo-Triassic (Tankard et al., 2009). The uplift implied from the AFT data  
864 represents the latest stage of landscape development to affect the region after  
865 denudation leading to exhumation of the mountain chain. Therefore, successively  
866 younger fission track ages towards the base of a mountain are to be expected as  
867 exhumation continues. Based on the above considerations, it is therefore argued that  
868 by the end of the Cretaceous the current watershed of the Gouritz catchment was  
869 mostly in place with the main trunk rivers active and depositing material offshore  
870 southern South Africa (Fig. 11).

871

872

873 5.4 *Where is the 'missing' sediment?*

874

875 Using the maximum exhumation values, ~ 11 km of exhumation has occurred across  
876 southern South Africa, with significant exhumation in the Early and Late Cretaceous,  
877 and the largest amount of exhumation over the CFB (Fig. 11). This is reasonable  
878 when considering the metamorphic grade of the Cape Supergroup (Frimmel et al.,  
879 2001). AFT studies also show large-scale denudation in the Mid-Late Cretaceous (~  
880 7 km, Tinker et al., 2008a). The discrepancy between the higher rates of exhumation  
881 stated here is considered to be due to the removal of an Early Cretaceous signature  
882 in many boreholes dated using AFT (e.g., Tinker et al., 2008a). Given this, and the  
883 offshore accumulations (e.g., Tinker et al., 2008b), it is highly likely that the  
884 additional 4km of exhumation occurred in the Early Cretaceous.

885 The maximum estimated volume of  $7.81 \times 10^5 \text{ km}^3$  material eroded from the southern  
886 drainage basins is larger than the volume of major long-lived submarine fan systems,  
887 such as the Amazon Fan, and if point-sourced would result in a fan up to 400 km  
888 long (e.g. Sømme et al., 2009) and kilometres thick. However, there is a major  
889 mismatch between the estimated onshore erosion and offshore accumulation of  
890 sediment. In the Outeniqua Basin and southern Outeniqua Basin, there is 268 500  
891  $\text{km}^3$  of material (Tinker et al., 2008b). Therefore,  $\sim 5.13 \times 10^5 \text{ km}^3$  (maximum) to  $\sim 2.53$   
892  $\times 10^5 \text{ km}^3$  (median) of sediment is unaccounted for (Table 5). If the southward  
893 draining catchments were active at least in the Early Cretaceous, the missing volume  
894 could have been transported deeper offshore via sediment gravity flows and  
895 hemipelagic processes (Tinker et al., 2008b).

896

897 During rifting, and the deposition of the Uitenhage Group, the Falkland Plateau was  
898 located offshore southern South Africa (Macdonald et al., 2003, Fig. 12). Adie (1952)  
899 first stated that the Falkland Plateau was in a rotated position east of South Africa,  
900 and formed part of the missing SE corner of the Karoo Basin. The amount and timing  
901 of Falkland Plateau rotation remains contentious (e.g., Richards et al., 1996;  
902 Macdonald et al., 2003; Stone et al., 2009; Richards et al., 2013) and is beyond the  
903 scope of this work. However, as the Falkland Plateau moved westward along the  
904 south side of the Falkland-Agulhus transform fault in the Late Jurassic to Early  
905 Cretaceous, the Falkland Plateau Basin developed (Macdonald et al., 2003; Fig. 12).  
906 The Falkland Plateau Basin formed the distal extension of the Pletmos and  
907 Bredasdorp basins in the early Aptian (Martin and Hartnady, 1986; Fouché et al.,  
908 1992; Ben-Avraham et al., 1993, 1997; Macdonald et al., 2003) or Albian (Ludwig,  
909 1983). A second phase of rifting occurred in the Early Cretaceous resulting in the  
910 North Falkland Basin, and the drifting apart of the plateau and the African continental  
911 plate (Richards et al., 1996; Fish, 2005; Fig. 12). Ludwig (1983) argued that the large  
912 change in depositional environment on the Maurice Bank from black shales to  
913 oxygenated nannofossil claystone is due to the plateau moving past the tip of Africa.

914

915 Taking an average of the scenarios presented in Table 7, during the break-up and  
916 rotation of the Falkland Plateau in the Early and Mid Cretaceous, when the plateau  
917 passed the tip of South Africa, a maximum of ~50% and minimum of ~20% (using  
918 the Scenarios in Table 7) of the exhumed material could have reached the plateau  
919 area (Fig. 12). This represents an average lithological thickness of 5.70 – 2.28 km for  
920 the maximum exhumation, and 1.75 – 0.7 km when constrained to the southern  
921 draining systems, and between 3.8 – 1.52 km for the median exhumation and 1.15 -

922 0.46 km when constrained to the southern draining systems in the median scenario.

923 Although drainage divides evolve over time, and all the scenarios show rates

924 increased in the Late Cretaceous, a significant volume of sediment was available to

925 be transported offshore and accreted to the Falkland Plateau (Fig. 12; 13).

926

927 Recent research on the Sea Lion Main Complex (SLMC) discovery in the North

928 Falkland Basin has identified an Early Cretaceous fluvial prodeltaic and turbidite

929 succession in a lacustrine syn-rift sequence (Farrimond et al., 2015; Griffiths, 2015).

930 The basin has large amounts of sand deposits (Bunt, 2015; Williams, 2015) and

931 comprise multiple basin-floor fans that offlap into a deep lake basin (Griffiths, 2015).

932  $U^{238}/Pb^{206}$  zircon ages suggest that the SLMC accumulated over <250 ka during the

933 early Aptian. If the Falkland Plateau was offshore southern South Africa with erosion

934 from the continent, and transverse and axial sediment routing then this

935 configuration could account for the large and rapid accumulations of sand in the syn-

936 rift lake basins (Fig. 12). The SL 10 and 20 fans are ~87 m thick and extend over

937 areas of 115 km<sup>2</sup> (Bunt, 2015). Extra-basinal material is predominantly coarse

938 material of volcanic and metamorphic origin, with rivers draining the sub-aerial

939 basement to the east (Williams, 2015). Williams (2015) states the Sea Lion Main

940 Complex sands are derived largely from a co-existing shallow water system, which

941 we postulate were supplied by the southerly draining river systems of southern South

942 Africa (Fig. 12). Several authors have commented on the similarity between the

943 stratigraphy of the Falkland Plateau Basin and the offshore Mesozoic basins of

944 southern South Africa (Martin et al., 1981; McMillian et al., 1997). Martin et al. (1981)

945 also argued that between the Late Jurassic and Early Cretaceous, during the rift to

946 drift period, the Bredasdorp, Pletmos Gamtoos, and Algoa basins were the proximal

947 tongues of the large Falkland Plateau Basin (Macdonald et al., 2003). In summary,  
948 we posit that the implication of this configuration is that a large proportion of the  
949 'missing' sediment eroded during the Late Jurassic and Early Cretaceous is  
950 represented by deposits in rift basins of the North Falkland Basin and the Falkland  
951 Plateau Basin. Further support comes from global sediment thickness maps (Divins,  
952 2003, Whittaker et al., 2013; Fig. 13). The Falkland Plateau is distinctive due to the  
953 thickness of sediment cover and lack of adjacent significant landmass, in contrast to  
954 southern South Africa (Fig. 13). This configuration means that the sedimentary  
955 basins are dislocated by ~6000 km from their drainage basins. This highlights the  
956 challenges of constraining and quantifying source-to-sink relationships in deep-time  
957 and close to active plate boundaries (Romans et al., 2009; Romans and Graham,  
958 2013).

959

## 960 **6. Conclusions**

961 A mismatch in the volumes of material eroded onshore and the volume of sediment  
962 deposited in offshore basins in the Mesozoic has been calculated. Large-scale  
963 exhumation (up to 11 km, since the Late Jurassic), initiated by rifting, resulted in the  
964 deposition of the Uitenhage Group in extensional basins, the only onshore  
965 representation of major landscape denudation. Integrating sedimentology,  
966 geomorphology and cosmogenic dating, evolutionary histories of two large-scale  
967 discordant basins in the Western Cape have been deciphered for the first time. The  
968 catchments had a complicated history and underwent multiple reorganisations due to  
969 stream capture in the Cretaceous. However, the main transverse trunk rivers of the  
970 catchments are long-lived features (up to 145 million years), resulting in extensive  
971 offshore sediment deposition. By reconstructing sediment routing patterns and

972 developing a range of exhumation scenarios tied to published AFT data, we interpret  
973 that the location for much of the 'missing' sediment is on the Falkland Plateau Basin,  
974 deposited during the Early Cretaceous when up to 50% of the sediment was  
975 available to be transported offshore. This represents a sediment sink has been has  
976 been separated from its source by 6000 km. In order to verify this, further work is  
977 needed to petrographically analyse the deposits on the Falkland Plateau. In addition,  
978 cosmogenic dating on drainage routing patterns will better constrain the onshore  
979 patterns of drainage evolution.

#### 980 Acknowledgments

981 We would like to thank the helpful and constructive reviews by Mark Wildman and  
982 Paul Green. The authors wish to thank the landowners in South Africa for access to  
983 outcrops and field assistant Sascha Eichenauer. The Council of Geoscience of  
984 South Africa are thanked for ArcGIS tiles of geology under the Academic/Research  
985 Licence Agreement. The British Geomorphology Society and the British  
986 Sedimentological Research Group are thanked for providing funding towards  
987 cosmogenic dating. Midland Valley Exploration Ltd. are thanked for providing the  
988 license for their proprietary software, Move.

#### 989 Reference list

- 990 Abdelkareem, M., El-Baz, F., 2015. Evidence of drainage reversal in the NE Sahara  
991 revealed by space-borne remote sensing data. *Journal of African Earth Sciences*,  
992 110, 245-257.
- 993 Abdelkareem, M., Ghoneim, E., El-Baz, F., Askalany, M., 2012. New insight on  
994 paleoriver development in the Nile basin of the eastern Sahara. *Journal of African*  
995 *Earth Sciences*, 62, 35-40.

- 996 Adams, S., Titus, R., Pietersen, K., Tredoux, G., Harris, C., 2001. Hydrochemical  
997 characteristics of aquifers near Sutherland in the Western Karoo, South Africa.  
998 *Journal of Hydrology*, 241, 91-103.
- 999 Adie, R.J., 1952. The position of the Falkland Islands in a reconstruction of  
1000 Gondwanaland. *Geological Magazine*, 89, 401-410.
- 1001 Babault, J., Van Den Driessche, J., Teixell, A., 2012. Longitudinal to transverse  
1002 drainage network evolution in the High Atlas (Morocco): The role of tectonics.  
1003 *Tectonics*, 31, TC4020.
- 1004 Bakker, E.M.V.Z., Mercer, J.H., 1986. Major late Cainozoic climatic events and  
1005 palaeoenvironmental changes in Africa viewed in a world wide context.  
1006 *Palaeogeography, Palaeoclimatology, Palaeoecology*, 56, 217-235.
- 1007 Balco, G., Stone, J.O., Lifton, N.A., Dunai, T.J., 2008. A complete and easily  
1008 accessible means of calculating surface exposure ages or erosion rates from 10 Be  
1009 and 26 Al measurements. *Quaternary geochronology*, 3, 174-195.
- 1010 Bellin, N., Vanacker, V., Kubik, P. W., 2014. Denudation rates and tectonic  
1011 geomorphology of the Spanish Betic Cordillera. *Earth and Planetary Science Letters*,  
1012 390, 19-30. Ben-Avraham, Z., Hartnady, C. J. H., Kitchin, K. A., 1997. Structure and  
1013 tectonics of the Agulhas-Falkland fracture zone. *Tectonophysics*, 282, 83-98.
- 1014 Ben-Avraham, Z., Hartnady, C. J. H., Malan, J. A., 1993. Early tectonic extension  
1015 between the Agulhas Bank and the Falkland Plateau due to the rotation of the  
1016 Lafonia microplate. *Earth and Planetary Science Letters*, 117, 43-58.
- 1017 Ben-Avraham, Z., Hartnady, C. J. H., Kitchin, K. A., 1997. Structure and tectonics of  
1018 the Agulhas-Falkland fracture zone. *Tectonophysics*, 282, 83-98. Bierman, P.R.,  
1019 1994. Using in situ produced cosmogenic isotopes to estimate rates of landscape  
1020 evolution: A review from the geomorphic perspective. *Journal of Geophysical*  
1021 *Research: Solid Earth*, 99, (B7), 13885-13896.
- 1022 Bierman, P.R., Caffee, M., 2001. Slow rates of rock surface erosion and sediment  
1023 production across the Namib Desert and escarpment, southern Africa. *American*  
1024 *Journal of Science*, 301, 326-358.
- 1025 Bierman, P.R., Nichols, K.K., Matmon, A., Enzel, Y., Larsen, J., Finkel, R., 2007. 10-  
1026 Be shows that Namibian drainage basins are slowly, steadily and uniformly eroding.  
1027 *Quaternary International*, 33, 167-168.
- 1028 Bierman, P.R., Reusser, L.J., Nichols, K.K., Matmon, A., Rood, D., 2009. Where is  
1029 the sediment coming from and where is it going - A 10Be examination of the northern  
1030 Queensland escarpment, Australia, 2009 Portland GSA Annual Meeting: Portland,  
1031 Oregon
- 1032

- 1033 Bierman, P.R., Coppersmith, R., Hanson, K., Neveling, J., Portenga, E.W., Rood,  
1034 D.H., 2014. A cosmogenic view of erosion, relief generation, and the age of faulting  
1035 in southern Africa. *GSA Today*, 24, 4-11.
- 1036
- 1037 Bishop, P., Hoey, T.B., Jansen, J.D., Artza, I.L., 2005. Knickpoint recession rate and  
1038 catchment area: the case of uplifted rivers in Eastern Scotland. *Earth Surface*  
1039 *Processes and Landforms*, 30, 767-778.
- 1040 Blumberg, D.G., Neta, T., Margalit, N., Lazar, M., Freilikher, V., 2004. Mapping  
1041 exposed and buried drainage systems using remote sensing in the Negev Desert,  
1042 Israel. *Geomorphology*, 61, 239-250.
- 1043 Bordy, E.M., America, T., 2016. Sedimentology of granite boulder conglomerates  
1044 and associated clastics in the onshore section of the late Mesozoic Pletmos Basin  
1045 (Western Cape, South Africa). *Journal of African Earth Sciences*, 119, 67-77.
- 1046 Breeze, P.S., Drake, N.A., Groucutt, H.S., Parton, A., Jennings, R.P., White, T.S.,  
1047 Clark-Balzan, L., Shipton, C., Scerri, E.M., Stimpson, C.M., Crassard, R., 2015.  
1048 Remote sensing and GIS techniques for reconstructing Arabian palaeohydrology and  
1049 identifying archaeological sites. *Quaternary International*, 382, 98-119.
- 1050 Brink, G.J., Keenan, J.H.G., 1993. Deposition of Fourth-Order, Post-Rift Sequences  
1051 and Sequence Sets, Lower Cretaceous (Lower Valanginian to Lower Aptian),  
1052 Pletmos Basin, Southern Offshore, South Africa: Chapter 3: Recent Applications of  
1053 Siliciclastic Sequence Stratigraphy. In: Weimer, P (Ed.) *Siliciclastic sequence*  
1054 *stratigraphy: recent developments and applications*. Vol. 58. Amer Assn of  
1055 *Petroleum Geologists*, 1993., pp. 43 - 69.
- 1056 Brocklehurst, S.H., Whipple, K.X., 2002. Glacial erosion and relief production in the  
1057 Eastern Sierra Nevada, California. *Geomorphology*, 42, 1–24. Broquet, C.A.M., 1992.  
1058 The sedimentary record of the Cape Supergroup: A review. In: de Wit, M.J.,  
1059 Ransome, I.G.D (Eds.) *Inversion tectonics of the Cape Fold Belt, Karoo and*  
1060 *Cretaceous basins of southern Africa.* ) A.A. Balkema, Rotterdam. pp. 159-  
1061 183. Brown, L.F. (Ed.). 1995. *Sequence Stratigraphy in Offshore South African*  
1062 *Divergent Basins: An Atlas on Exploration for Cretaceous Lowstand Traps* by Soekor  
1063 (Pty) Ltd, AAPG Studies in Geology 41. AAPG.
- 1064 Brown, R.W., Gallagher, K., Gleadow, A.J.W., Summerfield, M.A., 2000.  
1065 *Morphotectonic evolution of the South Atlantic margins of Africa and South America.*  
1066 In: Summerfield, M.A. (Ed.), *Geomorphology and Global Tectonics*. John Wiley and  
1067 *Sons Ltd.*, 255–284.
- 1068 Brown, R.W., Rust, D.J., Summerfield, M.A., Gleadow, A.J., De Wit, M.C., 1990. An  
1069 Early Cretaceous phase of accelerated erosion on the south-western margin of  
1070 Africa: Evidence from apatite fission track analysis and the offshore sedimentary

- 1071 record. *International Journal of Radiation Applications and Instrumentation. Part D.*  
1072 *Nuclear Tracks and Radiation Measurements*, 17, 339-350.
- 1073 Brown, R.W., Summerfield, M.A., Gleadow, A.J.W., 2002. Denudation history along  
1074 a transect across the Drakensberg Escarpment of southern Africa derived from  
1075 apatite fission track thermochronology. *Journal of Geophysical Research*, 107, B12
- 1076 Bunt, R.J., 2015. The use of seismic attributes for fan and reservoir definition in the  
1077 Sea Lion Field, North Falkland Basin. *Petroleum Geoscience*, 21, 137-149.
- 1078 Burbank, D., Meigs, A., Brozović, N., 1996. Interactions of growing folds and coeval  
1079 depositional systems. *Basin Research*, 8, 199-223.
- 1080 Burke, K., 1996. The African plate. *South African Journal of Geology*, 99, 341-409.
- 1081 Busk, H. G., 1929, *Earth flexures*. Cambridge Univ. Press (reprinted, 1957, by  
1082 William Trussell) 106 pp.
- 1083 Catuneanu, O., Wopfner, H., Eriksson, P.G., Cairncross, B., Rubidge, B.S., Smith,  
1084 R.M.H., Hancox, P.J., 2005. The Karoo basins of south-central Africa. *Journal of*  
1085 *African Earth Sciences*, 43, 211-253.
- 1086 Chadwick, O.A., Roering, J.J., Heimsath, A.M., Levick, S.R., Asner, G.P., Khomo, L.,  
1087 2013. Shaping post-orogenic landscapes by climate and chemical weathering.  
1088 *Geology*, 41, 1171-1174.
- 1089 Clapp, E. M., Bierman, P. R., Schick, A.P., Lekach, J., Enzel, Y., Caffee, M., 2000.  
1090 Sediment yield exceeds sediment production in arid region drainage basins.  
1091 *Geology*, 28, 995-998.
- 1092 Clift, P.D., Blusztajn, J., Nguyen, A.D., 2006. Large-scale drainage capture and  
1093 surface uplift in eastern Tibet–SW China before 24 Ma inferred from sediments of  
1094 the Hanoi Basin, Vietnam. *Geophysical Research Letters*, 33, L19403.
- 1095 Cockburn, H.A.P., Brown, R.W., Summerfield, M.A., Seidl, M.A., 2000. Quantifying  
1096 passive margin denudation and landscape development using a combined fission  
1097 track thermochronology and cosmogenic isotope analysis approach. *Earth and*  
1098 *Planetary Science Letters*, 179, 429–435.
- 1099 Codilean, A.T., Bishop, P., Stuart, F.M., Hoey, T.B., Fabel, D., Freeman, S.P., 2008.  
1100 Single-grain cosmogenic <sup>21</sup>Ne concentrations in fluvial sediments reveal spatially  
1101 variable erosion rates. *Geology*, 36, 159-162.
- 1102 Covault, J.A., Romans, B.W., Graham, S.A., Fildani, A., Hilley, G.E., 2011.  
1103 Terrestrial source to deep-sea sink sediment budgets at high and low sea levels:  
1104 Insights from tectonically active Southern California. *Geology*, 39, 619-622.

- 1105 Cox, K.G., 1989. The role of mantle plumes in the development of continental  
1106 drainage patterns. *Nature*, 342, 873-877.
- 1107 Dalton, T.J.S., Paton, D.A., Needham, T., Hodgson, N., 2015. Temporal and spatial  
1108 evolution of deepwater fold thrust belts: Implications for quantifying strain imbalance.  
1109 *Interpretation*, 3, SAA59-SAA70.
- 1110 Darvill, C.M., 2013. Cosmogenic nuclide analysis. *Geomorphological Techniques*,  
1111 Chapter 4, Section 2.10.
- 1112 Davis, W.M., 1889. A river-pirate. *Science*, 13, 108–109.
- 1113 Davis, W.M., 1906. The mountains of southernmost Africa. *Bulletin of the American*  
1114 *Geographical Society*, 38, 593-623.
- 1115 Decker, J.E., Niedermann, S., De Wit, M.J., 2011. Soil erosion rates in South Africa  
1116 compared with cosmogenic <sup>3</sup>He-based rates of soil production. *South African*  
1117 *Journal of Geology*, 114, 475-488.
- 1118 Decker, J.E., Niedermann, S., De Wit, M.J., 2013. Climatically influenced denudation  
1119 rates of the southern African plateau: Clues to solving a geomorphic paradox.  
1120 *Geomorphology*, 190, 48-60.
- 1121 de Wit, M.C.J., 1999. Post-Gondwana drainage and the development of diamond  
1122 placers in western South Africa. *Economic Geology*, 94, 721-740.
- 1123 de Wit, M., Marshall, T., Partridge, T., 2000. Fluvial deposits and drainage evolution.  
1124 In: *The Cenozoic of Southern Africa*, Partridge, T., Maud, R., (Eds) Oxford  
1125 monographs on geology and geophysics no. 40: NY
- 1126 de Wit, M.C.J., 2007. The Kalahari Epeirogeny and climate change: differentiating  
1127 cause and effect from core to space. *South African Journal of Geology*, 110, 367-  
1128 392.
- 1129 De Villiers, J., Jansen, H., Mulder, M.P., 1964. Die geologie van die gebied tussen  
1130 Worcester en Hermanus. Explanation Sheets 3319C (Worcester), 3419A (Caledon),  
1131 part of 3318D (Stellenbosch) and 3418B (Somerset West), *Geology Survey of South*  
1132 *Africa*, 69.
- 1133 Dingle, R.V., 1973. Mesozoic paleogeography of the Southern Cape, South Africa.  
1134 *Palaeogeography, Palaeoclimatology, Palaeoecology*, 13, 203-213.
- 1135 Dingle, R.V., Scrutton, R.A., 1974. Continental breakup and the development of  
1136 post-Paleozoic sedimentary basins around southern Africa. *Geological Society of*  
1137 *America Bulletin*, 85, 1467-1474.
- 1138 Dingle, R.V., Siesser, W.G., Newton, A.R. 1983. Mesozoic and Tertiary geology of  
1139 southern Africa. Rotterdam: Balkema. 375 pp. Dirks, P.H., Kibii, J.M., Kuhn, B.F.,

- 1140 Steininger, C., Churchill, S.E., Kramers, J.D., Pickering, R., Farber, D.L., Mériaux,  
1141 A.S., Herries, A.I., King, G.C., 2010. Geological setting and age of Australopithecus  
1142 sediba from southern Africa. *Science*, 328, 205-208.
- 1143 Divins, D.L., 2003. Total Sediment Thickness of the World's Oceans & Marginal  
1144 Seas, NOAA National Geophysical Data Center, Boulder, CO.
- 1145 Douglass, J., Meek, N., Dorn, R.I., Schmeeckle, M.W., 2009. A criteria-based  
1146 methodology for determining the mechanism of transverse drainage development,  
1147 with application to the southwestern United States. *Geological Society of America  
1148 Bulletin*, 121, 586-598.
- 1149 Douglass, J., Schmeeckle, M., 2007. Analogue modeling of transverse drainage  
1150 mechanisms. *Geomorphology*, 84, 22-43.
- 1151 Doucouré, C.M., de Wit, M.J., 2003. Old inherited origin for the present near-bimodal  
1152 topography of Africa. *Journal of African Earth Sciences*, 36, 371-388.
- 1153 Du Preez, J.W., 1944. Lithology, structure and mode of deposition of the Cretaceous  
1154 deposits in the Oudtshoorn area. *Annale van die Universiteit van Stellenbosch*, 22,  
1155 209-237.
- 1156 Durrheim, R.J., 1987. Seismic reflection and refraction studies of the deep structure  
1157 of the Agulhas Bank. *Geophysical Journal International*, 89, 395-398.
- 1158 Dury, G.H., 1960. Misfit streams: problems in interpretation, discharge, and  
1159 distribution. *Geographical Review*, 50, 219-242.
- 1160 Duxbury, J., 2009. Erosion rates in and around Shenandoah National Park, VA,  
1161 determined using analysis of cosmogenic <sup>10</sup>Be: University of Vermont, 134 pp.
- 1162 Ebinger, C.J., Sleep, N.H., 1998. Cenozoic magmatism throughout east Africa  
1163 resulting from impact of a single plume. *Nature*, 395, 788-791.
- 1164 Encarnación, J., Fleming, T.H., Elliot, D.H., Eales, H.V., 1996. Synchronous  
1165 emplacement of Ferrar and Karoo dolerites and the early breakup of Gondwana.  
1166 *Geology*, 24, 535-538.
- 1167 Erlanger, E.D., Granger, D.E., Gibbon, R.J., 2012. Rock uplift rates in South Africa  
1168 from isochron burial dating of fluvial and marine terraces. *Geology*, 40, 1019-1022.
- 1169 Fairbridge R.W., (ed). 1968. The encyclopaedia of geomorphology. Reinhold Book  
1170 Corporation, New York, 1296pp.
- 1171 Farrimond, P., Green, A., Williams, L.S., 2015. Petroleum geochemistry of the Sea  
1172 Lion Field, North Falkland Basin. *Petroleum Geoscience*, 21, 125-135.
- 1173 Fish, P., 2005. East Falkland basins reveal important exploration potential, *Oil and  
1174 Gas Journal*, 103, 34-40.

- 1175 Fleming, A., Summerfield, M.A., Stone, J.O., Fifield, L.K., Cresswell, R.G., 1999.  
1176 Denudation rates for the southern Drakensberg escarpment, SE Africa, derived from  
1177 in-situ-produced cosmogenic  $^{36}\text{Cl}$ : initial results. *Journal of the Geological Society*,  
1178 156, 209-212.
- 1179 Flint, S.S., Hodgson, D.M., Sprague, A.R., Brunt, R.L., Van der Merwe, W.C.,  
1180 Figueiredo, J., Prélat, A., Box, D., Di Celma, C., Kavanagh, J.P., 2011. Depositional  
1181 architecture and sequence stratigraphy of the Karoo basin floor to shelf edge  
1182 succession, Laingsburg depocentre, South Africa. *Marine and Petroleum Geology*,  
1183 28, 658-674.
- 1184 Flowers, R.M., Schoene, B., 2010. (U-Th)/He thermochronometry constraints on  
1185 unroofing of the eastern Kaapvaal craton and significance for uplift of the southern  
1186 African Plateau. *Geology*, 38, 827-830.
- 1187 Fouché, J., Bate, K. J., Van der Merwe, R., 1992. Plate tectonic setting of the  
1188 Mesozoic Basins, southern offshore, South Africa: A review. *Inversion tectonics of*  
1189 *the Cape Fold Belt, Karoo and Cretaceous basins of Southern Africa*, pp. 27-32.
- 1190 Frimmel, H.E., Fölling, P.G., Diamond, R., 2001. Metamorphism of the Permo-  
1191 Triassic Cape Fold Belt and its basement, South Africa. *Mineralogy and Petrology*,  
1192 73, 325-346.
- 1193 Gallagher, K., Brown, R., Johnson, C., 1998. Fission track analysis and its  
1194 applications to geological problems. *Annual Review of Earth and Planetary Science*,  
1195 26, 519-572.
- 1196 Gallagher, K., Brown, R., 1999. Denudation and uplift at passive margins: the record  
1197 on the Atlantic Margin of southern Africa. *Philosophical Transactions of the Royal*  
1198 *Society London*, 357, 835-859.
- 1199 Gawthorpe, R.L., Leeder, M.R., 2000. Tectono-sedimentary evolution of active  
1200 extensional basins. *Basin Research*, 12, 195-218.
- 1201 Ghosh, P., Sinha, S., Misra, A., 2015. Morphometric properties of the trans-  
1202 Himalayan river catchments: Clues towards a relative chronology of orogen-wide  
1203 drainage integration. *Geomorphology*. 223, 127-141.
- 1204 Gilbert, G.K., 1877. Report on the Geology of the Henry Mountains. US Government  
1205 Printing Office.
- 1206 Gilchrist, A.R., Kooi, H., Beaumont, C., 1994. Post-Gondwana geomorphic evolution  
1207 of southwestern Africa: Implications for the controls on landscape development from  
1208 observations and numerical experiments. *Journal of Geophysical Research: Solid*  
1209 *Earth*, 99, 12211-12228.

- 1210 Gleadow, A.J.W., Duddy, I.R., Lovering, J.F., 1983. Fission track analysis: A new  
1211 tool for the evaluation of thermal histories and hydrocarbon potential. Australian  
1212 Petroleum Exploration Association Journal, 23, 93-102.
- 1213 Gleadow, A.J.W., Duddy, I.R., Green, P.F., Lovering, J.F., 1986. Confined fission  
1214 track lengths in apatite: a diagnostic tool for thermal history analysis. Contributions to  
1215 Mineralogy and Petrology, 94, 405-415.
- 1216 Gosse, J.C., Phillips, F.M., 2001. Terrestrial in situ cosmogenic nuclides: theory and  
1217 application. Quaternary Science Reviews, 20, 1475-1560. Goudie, A. S., 2005. The  
1218 drainage of Africa since the Cretaceous. Geomorphology, 67, 437-456.
- 1219 Green, P.F., Duddy, I.R., Japsen, P., Bonow, J.M., Malan, J.A., 2016. Post-breakup  
1220 burial and exhumation of the southern margin of Africa. Basin Research. doi:  
1221 10.1111/bre.12167
- 1222 Griffin, D.L., 2006. The late Neogene Sahabi rivers of the Sahara and their climatic  
1223 and environmental implications for the Chad Basin. Journal of the Geological  
1224 Society, 163, 905-921.
- 1225 Griffiths, A., 2015. The reservoir characterization of the Sea Lion Field. Petroleum  
1226 Geoscience, 21, 199-209.
- 1227 Grosjean, A.S., Pittet, B., Gardien, V., Leloup, P.H., Mahéo, G., Barraza Garcia, J.,  
1228 2015. Tectonic heritage in drainage pattern and dynamics: the case of the French  
1229 South Alpine Foreland Basin (ca. 45–20 Ma). Basin Research, 1-25, pg 1-24, doi:  
1230 10.1111/bre.12134
- 1231 Gupta, A.K., Sharma, J.R., Sreenivasan, G., Srivastava, K.S., 2004. New findings on  
1232 the course of River Sarasvati. Journal of the Indian Society of Remote Sensing, 32,  
1233 1-24.
- 1234 Hancock, G.S., Anderson, R.S., Whipple, K.X., 1998. Beyond power: Bedrock river  
1235 incision process and form. In, Tinkler, K.J., Wohl, E (eds.) Rivers over rock: Fluvial  
1236 processes in bedrock channels, 107, American Geophysical Union, pp.35-60.
- 1237 Hansma, J., Tohver, E., Schrank, C., Jourdan, F., Adams, D., 2015. The timing of  
1238 the Cape Orogeny: New  $40\text{ Ar}/39\text{ Ar}$  age constraints on deformation and cooling of  
1239 the Cape Fold Belt, South Africa. Gondwana Research, 32, 122-137.
- 1240 Hanson, E.K., Moore, J.M., Bordy, E.M., Marsh, J.S., Howarth, G., Robey, J.V.A.,  
1241 2009. Cretaceous erosion in central South Africa: Evidence from upper-crustal  
1242 xenoliths in kimberlite diatremes. South African Journal of Geology, 112, 125-140.
- 1243 Harvey, A.M., Wells, S.G., 1987. Response of Quaternary fluvial systems to  
1244 differential epeirogenic uplift: Aguas and Feos river systems, southeast Spain.  
1245 Geology, 15, 689-693.

- 1246 Hattingh, J., 2008. Fluvial Systems and Landscape Evolution. In, Lewis, C. A.  
1247 Geomorphology of the Eastern Cape, South Africa. NISC.
- 1248 Haworth, R.J., Ollier, C.D., 1992. Continental rifting and drainage reversal: the  
1249 Clarence River of eastern Australia. *Earth Surface Processes and Landforms*, 17,  
1250 387-397.
- 1251 Hawthorne, J.B., 1975. Model of a kimberlite pipe. *Physics and Chemistry of the  
1252 Earth*, 9, 1-15.
- 1253 Heimsath, A., Chappel, J., Finkel, R.C., Fifield, K., Alimanovic, A., 2006. Escarpment  
1254 Erosion and Landscape Evolution in Southeastern Australia: Special Papers-  
1255 Geological Society of America, 398, 173.
- 1256 Heimsath, A.M., Fink, D., Hancock, G.R., 2009. The 'humped' soil production  
1257 function: eroding Arnhem Land, Australia. *Earth Surface Processes and Landforms*,  
1258 34, 1674-1684.
- 1259 Helland-Hansen, W., Sømme, T.O., Martinsen, O.J., Lunt, I., Thurmond, J., 2016.  
1260 Deciphering Earth's Natural Hourglasses: Perspectives On Source-To-Sink Analysis.  
1261 *Journal of Sedimentary Research*, 86, 1008-1033.
- 1262 Hewawasam, T., von Blanckenburg, F., Schaller, M., Kubik, P., 2003. Increase of  
1263 human over natural erosion rates in tropical highlands constrained by cosmogenic  
1264 nuclides. *Geology*, 31, 7, 597-600.
- 1265 Hill, R.S., 1972. The geology of the northern Algoa basin, Port Elizabeth. MSc thesis  
1266 (unpublished). University of Stellenbosch.
- 1267 Hirsch, K.K., Scheck-Wenderoth, M., van Wees, J.-D., Kuhlmann, G., 2010. Tectonic  
1268 subsidence history and thermal evolution of the Orange Basin. *Marine and  
1269 Petroleum Geology*, 27, 565-584.
- 1270 Hovius, N., 1996. Regular spacing of drainage outlets from linear mountain belts.  
1271 *Basin Research*, 8, 29-44.
- 1272 Humphrey, N.F., Konrad, S.K., 2000. River incision or diversion in response to  
1273 bedrock uplift. *Geology*, 28, 43-46.
- 1274 Hunt, C.B., 1969. Geologic history of the Colorado River. US Geological Survey  
1275 Professional Paper, 669, pp.59-130.
- 1276 Insel, N., Ehlers, T.A., Schaller, M., Barnes, J.B., Tawackoli, S., Poulsen, C.J., 2010.  
1277 Spatial and temporal variability in denudation across the Bolivian Andes from  
1278 multiple geochronometers. *Geomorphology*, 122, 65-77.
- 1279 Johnson, M.R., 1976. Stratigraphy and sedimentology of the Cape and Karoo  
1280 sequences in the Eastern Cape Province. Unpublished Thesis Rhodes University.

- 1281 Johnson, M.R. van Vuuren, C.J., Hegenberger, W.F., Rey, R., Shoko. U, 1996.  
1282 Stratigraphy of the Karoo Supergroup in South Africa: an overview. *Journal of*  
1283 *African Earth Sciences*, 23, 3-15.
- 1284 King, L.C., 1944. Geomorphology of the Natal Drakensberg. *Transactions of the*  
1285 *Geological Society of South Africa*, 47, 255-282.
- 1286 King, L.C., 1953. Cannons of landscape evolution. *Geology Society of America*  
1287 *Bulletin*, 64, 721-752.
- 1288 King, L.C., 1966. The origin of bornhardts. *Zeitschrift fur Geomorphologie*, 10, 97–98
- 1289 King, R.C. 2005. The structural evolution of the Cape Fold Belt and southwest Karoo  
1290 Basin: Implications on sediment storage and routing to the southwest Karoo Basin,  
1291 South Africa: Unpublished Ph.D. thesis. University of Liverpool, 327p.
- 1292 King, R.C., Hodgson, D.M., Flint, S.S., Potts, G.J., Van Lente, B. 2009. Development  
1293 of subaqueous fold belts as a control on the timing and distribution of deepwater  
1294 sedimentation: an example from the southwest Karoo Basin, South Africa. In,  
1295 Kneller, B.C., Martinsen, O.J., McCaffrey, W.D. (Eds.), *External Controls on Deep-*  
1296 *Water Depositional Systems*. SEPM, Special Publication, 92, 261–278
- 1297 Kounov, A., Niedermann, S., de Wit, M.J., Viola, G., Andreoli, M., Erzinger, J., 2007.  
1298 Present denudation rates at selected sections of the South African escarpment and  
1299 the elevated continental interior based on cosmogenic  $^3\text{He}$  and  $^{21}\text{Ne}$ . *South African*  
1300 *Journal of Geology*, 110, 235-248.
- 1301 Kounov, A., Viola, G., De Wit, M., Andreoli, M.A.G., 2009. Denudation along the  
1302 Atlantic passive margin: new insights from apatite fission-track analysis on the  
1303 western coast of South Africa. In, Lisker, F., Ventura, B., Glasmacher, U.A. (Eds.)  
1304 *Thermochronological Methods: From Palaeotemperature Constraints to Landscape*  
1305 *Evolution Models*. Geological Society, London, Special Publications, 324, 287-306
- 1306 Kounov, A., Niedermann, S., de Wit, M.J., Codilean, A.T., Viola, G., Andreoli, M.,  
1307 Christl, M., 2015. Cosmogenic  $^{21}\text{Ne}$  and  $^{10}\text{Be}$  reveal a more than 2 Ma alluvial fan  
1308 flanking the Cape Mountains, South Africa. *South African Journal of Geology*, 118,  
1309 129-144.
- 1310 Kubik, P.W., Christl, M., 2010.  $^{10}\text{Be}$  and  $^{26}\text{Al}$  measurements at the Zurich 6MV  
1311 Tandem AMS facility. *Nuclear Instruments and Methods in Physics Research*  
1312 *Section B: Beam Interactions with Materials and Atoms*, 268, 880-883.
- 1313 Leeder, M.R., Gawthorpe, R.L., 1987. Sedimentary models for extensional tilt-  
1314 block/half-graben basins. In, Coward, M.P., Dewey, J.F., Hanacok, P.I. (Eds.)  
1315 *Continental Extensional Tectonics* Geological Society, London, Special Publications,  
1316 28, 139-152.

- 1317 Lock, B.E., Shone, R., Coates, A. T., Hatton, C. J., 1975. Mesozoic Newark type  
1318 sedimentation within the Cape Fold Belt of South Africa. Proceedings of the 9<sup>th</sup>  
1319 International Congress of Sedimentology, Nice 1975, 2, 217-225.
- 1320 Ludwig, W.J., 1983, Geologic framework of the Falkland Plateau: Initial reports  
1321 DSDP, Leg 71, Valparaiso to Santos, 1980, 281–293.
- 1322 Macdonald, D., Gomez-Perez, I., Franzese, J., Spalletti, L., Lawver, L., Gahagan, L.,  
1323 Dalziel, I., Thomas, C., Trewin, N., Hole, M., Paton, D., 2003. Mesozoic break-up of  
1324 SW Gondwana: implications for regional hydrocarbon potential of the southern South  
1325 Atlantic. *Marine and Petroleum Geology*, 20, 287-308.
- 1326 Macgregor, D.S., 2012. The development of the Nile drainage system: integration of  
1327 onshore and offshore evidence. *Petroleum Geoscience*, 18, 417-431.
- 1328 Martin, A.K., Hartnady, C.J., Goodlad, S.W., 1981. A revised fit of South America  
1329 and south central Africa. *Earth and Planetary Science Letters*, 54, 293-305.
- 1330 Martin, A.K., Hartnady, C.J.H., 1986. Plate tectonic development of the South West  
1331 Indian Ocean: a revised reconstruction of East Antarctica and Africa. *Journal of*  
1332 *Geophysical Research: Solid Earth*, 91, 4767-4786.
- 1333 Maske, S., 1957, A critical review of superimposed and antecedent rivers in southern  
1334 Africa. In: *Annals of the University of Stellenbosch: Series A*, 33, 1-22.
- 1335 Matmon, A.S., Bierman, P., Larsen, J., Southworth, S., Pavich, M., Finkel, R.,  
1336 Caffee, M., 2003. Erosion of an ancient mountain range, the Great Smoky  
1337 Mountains, North Carolina and Tennessee. *American Journal of Science*, 303, 817-  
1338 855. Maw, G., 1866. Notes on the comparative structure of surfaces produced by  
1339 sub-aerial and marine denudation. *Geological Magazine*, 3, 439–451.
- 1340 McCauley, J.F., Breed, C.S., Schaber, G.G., McHugh, W.P., Issawi, B., Haynes,  
1341 C.V., Grolier, M.J., Kilani, A.E., 1986. Paleodrainages of the Eastern Sahara-The  
1342 Radar Rivers Revisited (SIR-A/B Implications for a Mid-Tertiary Trans-African  
1343 Drainage System). *IEEE Transactions on Geoscience and Remote Sensing*, 4, 624-  
1344 648.
- 1345 McHugh, W.P., McCauley, J.F., Haynes, C.V., Breed, C.S., Schaber, G.G., 1988.  
1346 Paleorivers and Geoarchaeology in the southern Egyptian Sahara. *Geoarchaeology*,  
1347 3, 1-40.
- 1348 McLachlan, I.R., McMillan, I.K., 1976. Review and stratigraphic significance of  
1349 southern Cape Mesozoic palaeontology. *Transactions of the Geology Society of*  
1350 *South Africa*, 79, 197-212.
- 1351 McMillan, I.K., Brink, G.I., Broad, D.S., Maier, J.J., 1997. Late Mesozoic sedimentary  
1352 basins off the south coast of South Africa. *Sedimentary Basins of the World*, 3, 319-  
1353 376.

- 1354 Moore, A., Blenkinsop, T., 2002. The role of mantle plumes in the development of  
1355 continental-scale drainage patterns: The southern African example revisited. South  
1356 African Journal of Geology, 105, 353-360.
- 1357 Moore, A., Blenkinsop, T., 2006. Scarp retreat versus pinned drainage divide in the  
1358 formation of the Drakensberg escarpment, southern Africa. South African Journal of  
1359 Geology, 109, 599-610.
- 1360 NASA Reverb. 2015. <http://reverb.echo.nasa.gov/reverb/>
- 1361 Nyblade, A.A., Sleep, N.H., 2003. Long lasting epeirogenic uplift from mantle plumes  
1362 and the origin of the Southern African Plateau. Geochemistry, Geophysics,  
1363 Geosystems, 4, 1-29.
- 1364 Oberlander, M., 1985. Origin of drainage transverse to structures in orogens. In:  
1365 Morisawa, M., Hack, J.T (Eds.) Tectonic Geomorphology , Allen & Unwin, Boston.  
1366 pp. 155-182.
- 1367 Ouimet, W.B., Whipple, K.X., Crosby, B.T., Johnson, J.P., Schildgen, T.F., 2008.  
1368 Epigenetic gorges in fluvial landscapes. Earth Surface Processes and Landforms,  
1369 33, 1993 – 2009.
- 1370 Partridge, T.C., 1998. Of diamonds, dinosaurs and diastrophism: 150 million years of  
1371 landscape evolution in southern Africa. South African Journal of Geology, 101, 165–  
1372 184.
- 1373 Partridge, T.C., Maud, R.R., 1987. Geomorphic evolution of southern Africa since the  
1374 Mesozoic. South African Journal of Geology, 90, 179-208.
- 1375 Partridge, T.C., Dollar, E.S.J., Moolman, J., Dollar, L.H., 2010. The geomorphic  
1376 provinces of South Africa, Lesotho and Swaziland: A physiographic subdivision for  
1377 earth and environmental scientists. Transactions of the Royal Society of South  
1378 Africa, 65, 1-47.
- 1379 Paton, D.A., 2002. The evolution of southern South Africa. Insights into structural  
1380 inheritance and heterogeneous normal fault growth. Unpublished PhD Thesis,  
1381 University of Edinburgh.
- 1382 Paton, D.A., 2006. Influence of crustal heterogeneity on normal fault dimensions and  
1383 evolution: southern South Africa extensional system. Journal of Structural Geology,  
1384 28, 868-886.
- 1385 Paton, D., 2011. Post-Rift Deformation of the North East and South Atlantic Margins:  
1386 Are “Passive Margins” Really Passive? In: Busby, C., Azor, A., (Eds.) Tectonics of  
1387 Sedimentary Basins: Recent Advances, John Wiley & Sons, Ltd, Chichester, UK.
- 1388

- 1389 Paton, D.A., Underhill, J.R., 2004. Role of crustal anisotropy in modifying the  
1390 structural and sedimentological evolution of extensional basins: the Gamtoos Basin,  
1391 South Africa. *Basin Research*, 16, 339-359. Paton, D.A., Macdonald, D.I., Underhill,  
1392 J.R., 2006. Applicability of thin or thick skinned structural models in a region of  
1393 multiple inversion episodes; southern South Africa. *Journal of Structural Geology*,  
1394 28, 1933-1947.
- 1395
- 1396 Paton, DA; van der Spuy, D; di Primio, R; Horsfield, B., 2008. Tectonically induced  
1397 adjustment of passive margin accommodation space; influence on the hydrocarbon  
1398 potential of the Orange Basin, South Africa. *AAPG Bulletin*, 92, 589-609.
- 1399 Quigley, M., Sandiford, M., Fifield, K., Alimanovic, A., 2007, Bedrock erosion and  
1400 relief production in the northern Flinders Ranges, Australia: *Earth Surface Processes*  
1401 *and Landforms*, 32, 929 - 944.
- 1402 Rabassa, J., 2010. Gondwana paleolandscapes: long-term landscape evolution,  
1403 genesis, distribution and age. *Geociências (São Paulo)*, 29, 541-570.
- 1404 Ramasamy, S.M., Bakliwal, P.C., Verma, R.P., 1991. Remote sensing and river  
1405 migration in Western India. *Remote Sensing*, 12, 2597-2609.
- 1406 Ramsey, L.A., Walker, R.T., Jackson, J., 2008. Fold evolution and drainage  
1407 development in the Zagros mountains of Fars province, SE Iran. *Basin Research*,  
1408 20, 23-48.
- 1409 Rastall, R. H., 1911. The Geology of the Districts of Worcester, Robertson, and  
1410 Ashton (Cape Colony). *Quarterly Journal of the Geological Society*, 67, 701-733.
- 1411 Richards, P.C., Gatliff, R.W., Quinn, M.F., Fannin, N.G.T., Williamson, J.P., 1996.  
1412 The geological evolution of the Falkland Islands continental shelf. In: B.C. Storey,  
1413 E.C. King, R.A. Livermore (Eds.), *Weddell Sea Tectonics and Gondwana Break-up*.  
1414 Geological Society, London, Special Publications, 108, 05-128.
- 1415 Richards, P.C., Stone, P., Kimbell, G.S., McIntosh, W.C., Phillips, E.R., 2013.  
1416 Mesozoic magmatism in the Falkland Islands (South Atlantic) and their offshore  
1417 sedimentary basins. *Journal of Petroleum Geology*, 36, 61-73.
- 1418 Richardson, J.C., Hodgson, D.M., Wilson, A., Carrivick, J.L., Lang, A., 2016. Testing  
1419 the applicability of morphometric characterisation in discordant catchments to  
1420 ancient landscapes: A case study from southern Africa. *Geomorphology*, 261, 162-  
1421 176.
- 1422 Rigassi, D. A., Dixon, G. E. 1972. Cretaceous of the Cape Province, Republic of  
1423 South Africa. *Ibadan University Conference on African Geology*, 170, 513-527.

- 1424 Roberts, G.G., Paul, J.D., White, N., Winterbourne, J., 2012. Temporal and spatial  
1425 evolution of dynamic support from river profiles: A framework for Madagascar.  
1426 *Geochemistry, Geophysics, Geosystems*, 13, 1-23.
- 1427 Roberts, G.G., White, N., 2010. Estimating uplift rate histories from river profiles  
1428 using African examples. *Journal of Geophysical Research: Solid Earth*, 115(B2), 1-  
1429 24.
- 1430 Rogers, C. A., 1903. The geological history of the Gouritz River system.  
1431 *Transactions of the South African Philosophical Society*, 14, 375-384.
- 1432 Romans, B.W., Graham, S.A., 2013. A deep-time perspective of land-ocean linkages  
1433 in the sedimentary record. *Annual Review of Marine Science*, 5, 69-94.
- 1434 Romans, B.W., Normark, W.R., McGann, M.M., Covault, J.A., Graham, S.A., 2009.  
1435 Coarse-grained sediment delivery and distribution in the Holocene Santa Monica  
1436 Basin, California: implications for evaluating source-to-sink flux at millennial time  
1437 scales. *Geological Society of America Bulletin*, 121, 1394-1408.
- 1438 Rowsell, D., De Swardt, A., 1976. Diagenesis in Cape and Karoo sediments, South  
1439 Africa, and its bearing on their hydrocarbon potential. *Transactions of the Geological  
1440 Society of South Africa*, 79, 81-145.
- 1441 Rudge, J.F., Roberts, G.G., White, N.J. and Richardson, C.N., 2015. Uplift histories  
1442 of Africa and Australia from linear inverse modeling of drainage inventories. *Journal  
1443 of Geophysical Research: Earth Surface*, 120, 894-914.
- 1444 Rust, D. J., Summerfield, M.  
1445 A., 1990. Isopach and borehole data as indicators of rifted margin evolution in  
1446 southwestern Africa. *Marine and Petroleum Geology*, 7, 277-287.
- 1446 Scharf, T.E., Codilean, A.T., De Wit, M., Jansen, J.D., Kubik, P.W., 2013. Strong  
1447 rocks sustain ancient postorogenic topography in southern Africa. *Geology*, 41, 331-  
1448 334.
- 1449 Schlische, R.W., 1992. Structural and stratigraphic development of the Newark  
1450 extensional basin, eastern North America: Evidence for the growth of the basin and  
1451 its bounding structures. *Geological Society of America Bulletin*, 104, 1246-1263.
- 1452 Seidl, M., Dietrich W.E., Kirchner J.W., 1994. Longitudinal profile development into  
1453 bedrock: an analysis of Hawaiian channels. *Journal of Geology*, 102, 457-74.
- 1454 Seidl, M.A., Finkel, R.C., Caffee, M.W., Hudson, G.B., Dietrich, W.E., 1997.  
1455 Cosmogenic isotope analyses applied to river longitudinal profile evolution: problems  
1456 and interpretations. *Earth Surface Processes and Landforms*, 22, 195-209
- 1457 Shone, R.W., 1978. A case for lateral gradation between the Kirkwood and Sundays  
1458 River Formations, Algoa Basin. *Transactions of Geology Society of South Africa*, 81,  
1459 319- 326.

- 1460 Shone, R.W., 2006. Onshore post-Karoo Mesozoic deposits. In: Johnson, M.R.,  
1461 Anhaeusser, C.R., Thomas, R.J. (Eds.) The geology of South Africa, Geological  
1462 Society of South Africa, Marshalltown. pp. 541-552.
- 1463 Shone, R.W., Booth, P.W.K., 2005. The Cape Basin, South Africa: A review. Journal  
1464 of African Earth Sciences, 43, 196-210.
- 1465 Söhnge, P. G., 1934. The Worcester fault. Transactions of geology Society of South  
1466 Africa, 37, 253-277.
- 1467 Sømme, T.O., Helland-Hansen, W., Martinsen, O.J., Thurmond, J.B., 2009.  
1468 Relationships between morphological and sedimentological parameters in source-to-  
1469 sink systems: a basis for predicting semi-quantitative characteristics in subsurface  
1470 systems. Basin Research, 21, 361-387.
- 1471 Sømme, T.O., Jackson, C.A.L., 2013. Source-to-sink analysis of ancient sedimentary  
1472 systems using a subsurface case study from the Møre-Trøndelag area of southern  
1473 Norway: Part 2—sediment dispersal and forcing mechanisms. Basin Research, 25,  
1474 512-531.
- 1475 Sonibare, W.A., Sippel, J., Scheck-Wenderoth, M., Mikeš, D., 2015. Crust-scale 3D  
1476 model of the Western Bredasdorp Basin (Southern South Africa): data-based  
1477 insights from combined isostatic and 3D gravity modelling. Basin Research, 27, 125-  
1478 151.
- 1479 Stankiewicz, J., Ryberg, T., Schulze, A., Lindeque, A., Weber, M.H., De Wit, M.J.,  
1480 2007. Initial results from wide-angle seismic refraction lines in the southern Cape.  
1481 South African Journal of Geology, 110, 407-418.
- 1482 Stanley, J.R., Flowers, R.M., Bell, D.R., 2013. Kimberlite (U-Th)/He dating links  
1483 surface erosion with lithospheric heating, thinning, and metasomatism in the  
1484 southern African Plateau. Geology, 41, 1243-1246. Stock, J.D., Montgomery, D.R.,  
1485 1999. Geologic constraints on bedrock river incision using the stream power law.  
1486 Journal of Geophysical Research B, 104, 4983-4993.
- 1487 Stokes, M., Mather, A.E., 2003. Tectonic origin and evolution of a transverse  
1488 drainage: the Rio Almanzora, Betic Cordillera, Southeast Spain. Geomorphology, 50,  
1489 59-81.
- 1490 Stokes, M., Mather, A.E., Belfoul, A., Farik, F., 2008. Active and passive tectonic  
1491 controls for transverse drainage and river gorge development in a collisional  
1492 mountain belt (Dades Gorges, High Atlas Mountains, Morocco). Geomorphology,  
1493 102, 2-20.
- 1494 Stone, P., Kimbell, G.S., Richards, P.C., 2009. Rotation of the Falklands microplate  
1495 reassessed after recognition of discrete Jurassic and Cretaceous dyke swarms.

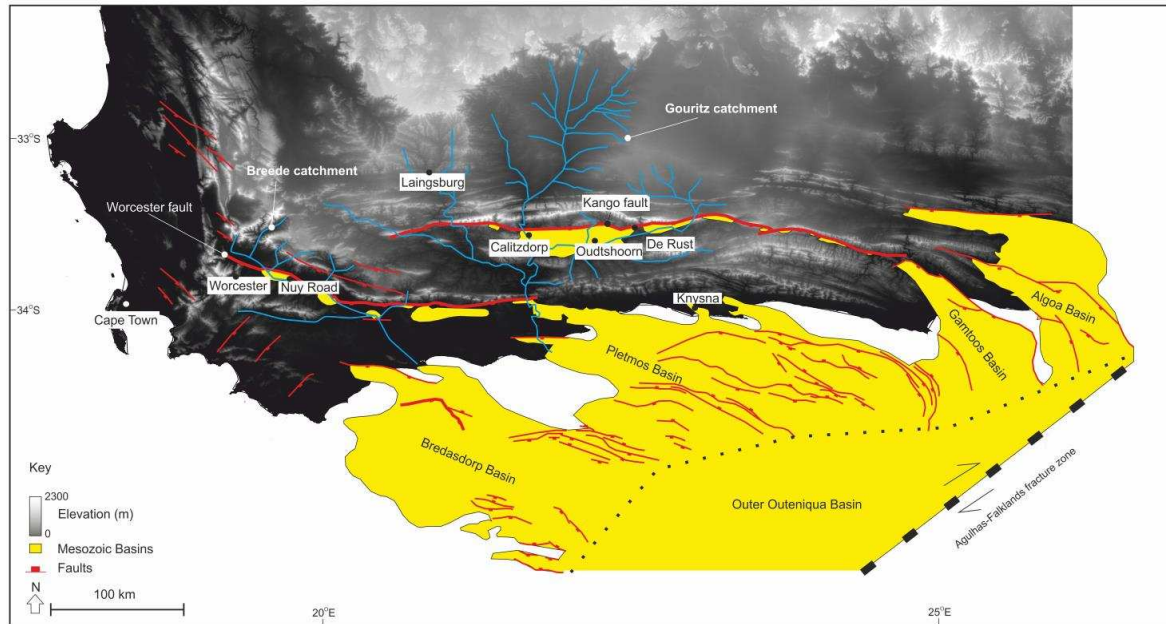
- 1496 Petroleum Geoscience, 15, 279-287. Summerfield, M.A., 1991. Global  
1497 geomorphology. Routledge. 537 pp.
- 1498 Szwarc, T.S., Johnson, C.L., Stright, L.E., McFarlane, C.M., 2015. Interactions  
1499 between axial and transverse drainage systems in the Late Cretaceous Cordilleran  
1500 foreland basin: Evidence from detrital zircons in the Straight Cliffs Formation,  
1501 southern Utah, USA. Geological Society of America Bulletin, 127, 372-392.
- 1502 Tankard, A., Welsink, H., Aukes, P., Newton, R., Stettler, E., 2009. Tectonic  
1503 evolution of the Cape and Karoo basins of South Africa. Marine and Petroleum  
1504 Geology, 26, 1379-1412.
- 1505 Thomson, K., 1999. Role of continental break-up, mantle plume development and  
1506 fault reactivation in the evolution of the Gamtoos Basin, South Africa. Marine and  
1507 Petroleum Geology, 16, 409-429.
- 1508 Tinker, J., 2005. Quantifying South African Uplift: using apatite fission track  
1509 thermochronology and offshore sediment volumes to test the balance between  
1510 denudation (onshore) and deposition (offshore) since Gondwana break-up.  
1511 Unpublished PhD thesis, Cape Town University.
- 1512 Tinker, J., de Wit, M., Brown, R. 2008a. Mesozoic exhumation of the southern Cape,  
1513 South Africa, quantified using apatite fission track thermochronology.  
1514 Tectonophysics, 455, 77-93.
- 1515 Tinker, J., de Wit, M., Brown, R. 2008b. Linking source and sink: Evaluating the  
1516 balance between onshore erosion and offshore sediment accumulation since  
1517 Gondwana break-up, South Africa. Tectonophysics, 455, 94-103.
- 1518 Twidale, C., 2004. River patterns and their meaning. Earth-Science Reviews, 67,  
1519 159-218.
- 1520 Visser, J. N. J., 1984. A review of the Stormberg Group and Drakensberg volcanics  
1521 in southern Africa. Palaeontologica Africana, 25, 5-27.
- 1522 Von Blanckenburg, F., Belshaw, N., O'Nions, R., 1996. Separation of  $^9\text{Be}$  and  
1523 cosmogenic  $^{10}\text{Be}$  from environmental materials and SIMS isotope dilution analysis.  
1524 Chemical Geology 129, 93–99.
- 1525 Von Blanckenburg, F., Hewawasam, T., Kubik, P.W., 2004. Cosmogenic nuclide  
1526 evidence for low weathering and denudation in the wet, tropical highlands of Sri  
1527 Lanka. Journal of Geophysical Research: Earth Surface, 109 (F3).
- 1528 Von Blanckenburg, F., Willenbring, J. K., 2014. Cosmogenic nuclides: Dates and  
1529 rates of Earth-surface change. Elements, 10, 341-346.
- 1530 van der Beek, P., Summerfield, M.A., Braun, J., Brown, R.W., Fleming, A., 2002.  
1531 Modeling postbreakup landscape development and denudational history across the

- 1532 southeast African (Drakensberg Escarpment) margin. *Journal of Geophysical*  
1533 *Research: Solid Earth*, 107(B12).
- 1534 Van der Wateren, F.M., Dunai, T.J., 2001. Late Neogene passive margin denudation  
1535 history—cosmogenic isotope measurements from the central Namib desert. *Global*  
1536 *and Planetary Change*, 30, 271-307.
- 1537 Weissel J.K., Seidl M.A., 1998. Inland propagation of erosional escarpments and  
1538 river profile evolution across the southeastern Australian passive continental margin.  
1539 In, Tinkler, K.J., Wohl, E (eds.) *Rivers over rock: Fluvial processes in bedrock*  
1540 *channels*, 107, American Geophysical Union, pp.189–206.
- 1541 Whittaker, A.C., Boulton, S.J., 2012. Tectonic and climatic controls on knickpoint  
1542 retreat rates and landscape response times. *Journal of Geophysical Research: Earth*  
1543 *Surface*, 117(F2).
- 1544 Whittaker, J., Goncharov, A., Williams, S., Muller, R.D., Leitchenkov, G., 2013.  
1545 Global sediment thickness data set updated for the Australian-Antarctic Southern  
1546 Ocean. *Geochemistry, Geophysics, Geosystems*, 14, 3297–3305,  
1547 doi:10.1002/ggge.20181.
- 1548 Wildman, M., Brown, R., Watkins, R., Carter, A., Gleadow, A., Summerfield, M.,  
1549 2015. Post break-up tectonic inversion across the southwestern cape of South  
1550 Africa: New insights from apatite and zircon fission track thermochronometry.  
1551 *Tectonophysics*, 654, 30-55.
- 1552 Wildman, M., Brown, R., Beucher, R., Persano, C., Stuart, F., Gallagher, K.,  
1553 Schwanethal, J., Carter, A., 2016. The chronology and tectonic style of landscape  
1554 evolution along the elevated Atlantic continental margin of South Africa resolved by  
1555 joint apatite fission track and (U-Th-Sm)/He thermochronology. *Tectonics*. 35,  
1556 doi:10.1002/ 2015TC004042.
- 1557 Williams, L.S., 2015. Sedimentology of the Lower Cretaceous reservoirs of the Sea  
1558 Lion Field, North Falkland Basin. *Petroleum Geoscience*, 21, 183-198.
- 1559 Winter, H. De la R. 1973. Geology of the Algoa Basin, South Africa. *Sedimentary*  
1560 *Basins of the African Coasts*, Association of Africa Geology Survey, Paris, 2nd part  
1561 (south and east coasts), 17-48.
- 1562 Wohl E.E., Greenbaum N, Schick A.P., Baker V.R., 1994. Controls on bedrock  
1563 channel incision along Nahal Paran, Israel. *Earth Surface Processes and Landforms*,  
1564 19, 1–13
- 1565 Youssef, A.M., 2009. Mapping the mega paleodrainage basin using shuttle radar  
1566 topography mission in Eastern Sahara and its impact on the new development  
1567 projects in Southern Egypt. *Geo-spatial Information Science*, 12, 182-190.
- 1568

1569 Figures

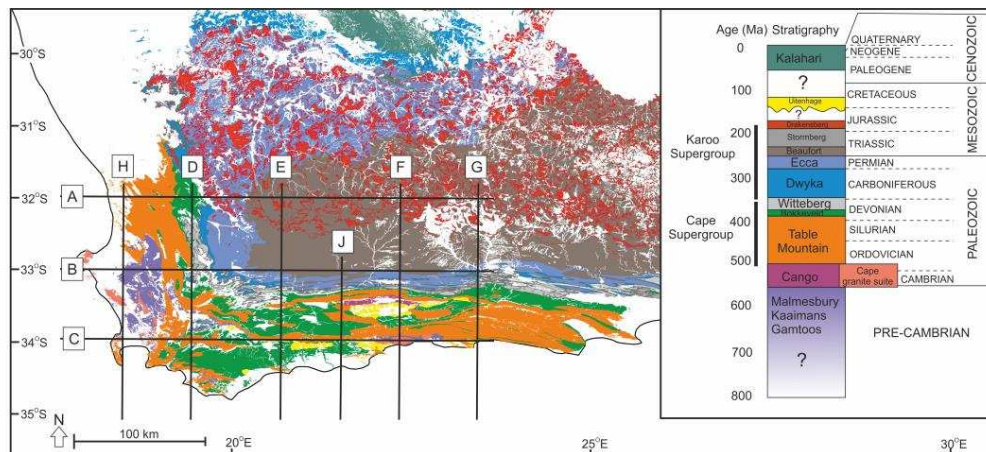
1570

1571 Figure 1 – Location map of study sites and Mesozoic basins of southern South  
 1572 Africa, adapted from McMillan et al. (1997). The current day planforms of the Breede  
 1573 and Gouritz catchments are shown.



1574

1575 Figure 2 – Geological map of southern South Africa showing key stratigraphic units  
 1576 used in the cross section construction. The current day distribution of the  
 1577 Drakensberg volcanics are towards the north. The cross sectional locations A-J are  
 1578 also displayed.



1579

1580

1581 Figure 3 – The Gouritz River current catchment planform and trunk river location; the

1582 main trunk river transect the Cape Fold Belt, and do not exploit structural

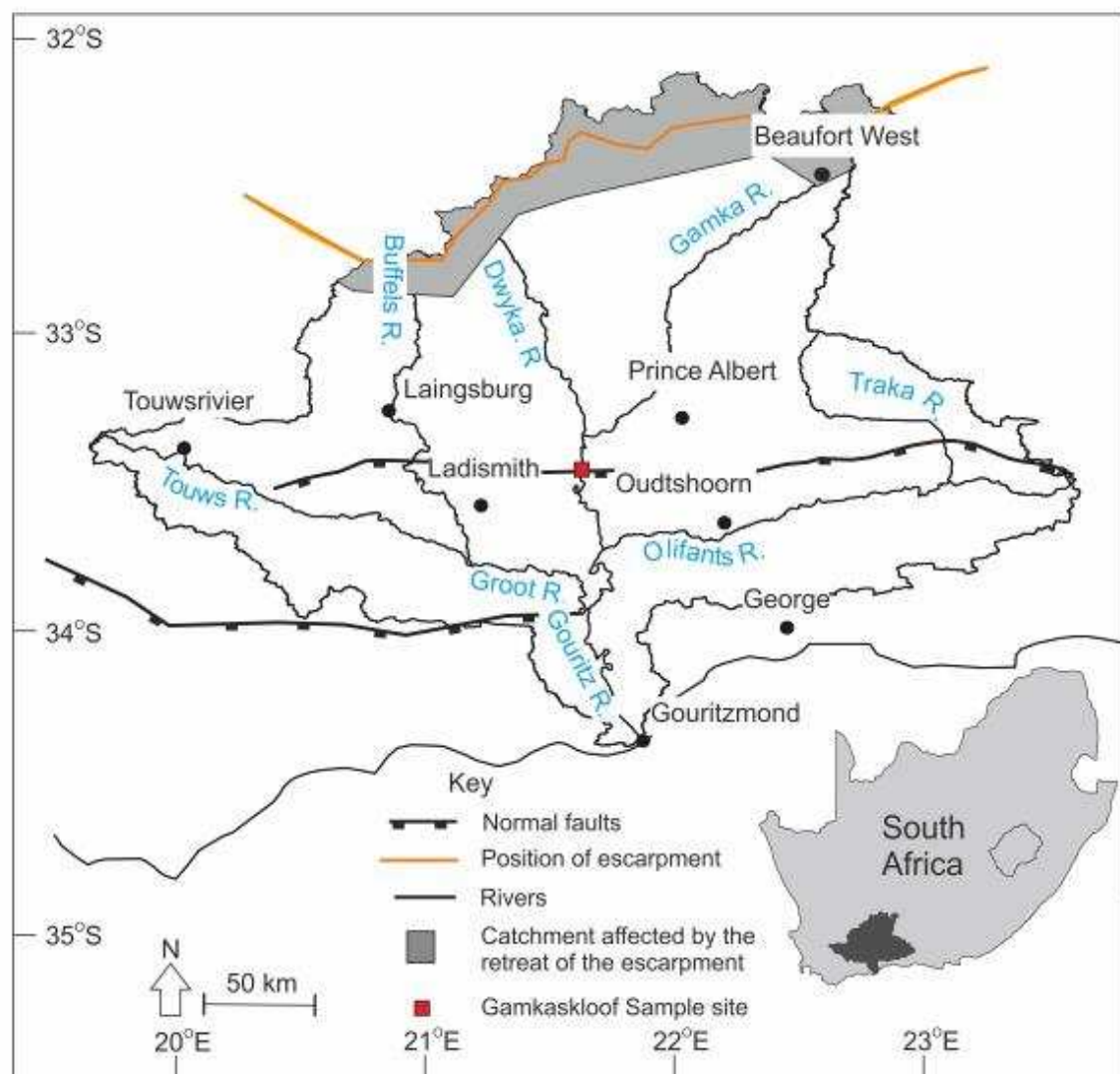
1583 weaknesses. Many of the headwater streams within the catchment dissect the Great

1584 Escarpment, further stream capture in this location will increase the drainage area of

1585 the Gouritz catchment and reduce the catchment area of the Orange River. The

1586 sample location of the cosmogenic sample can be observed, which is also shown on

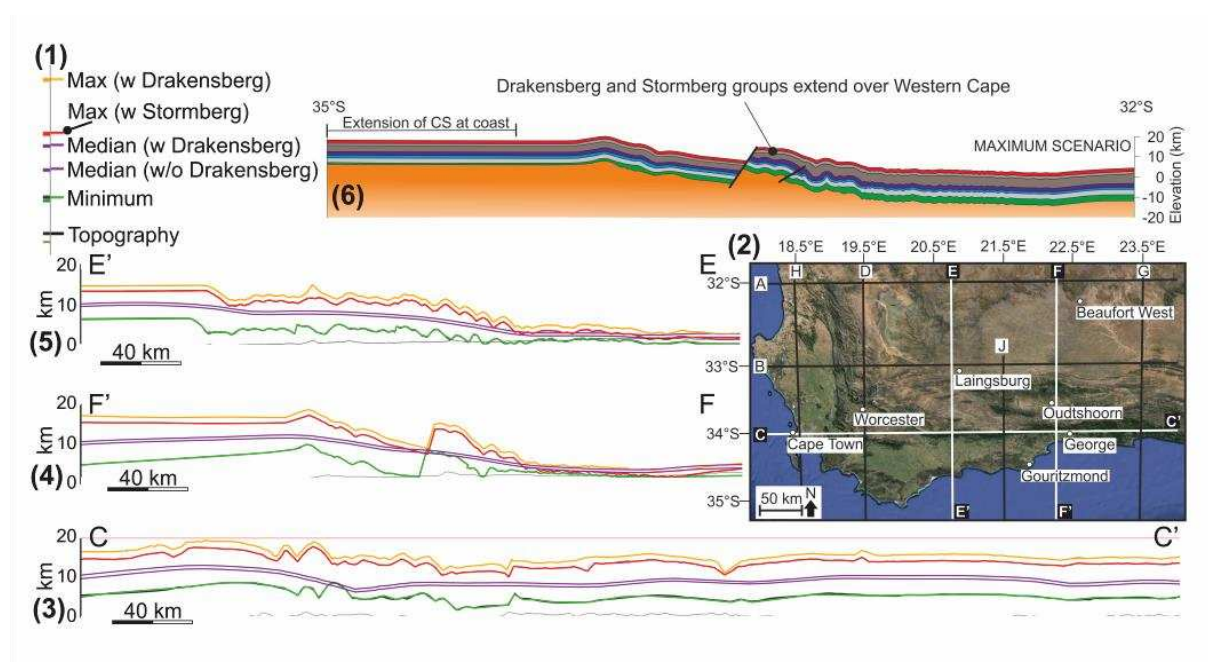
1587 Fig. 6.



1588

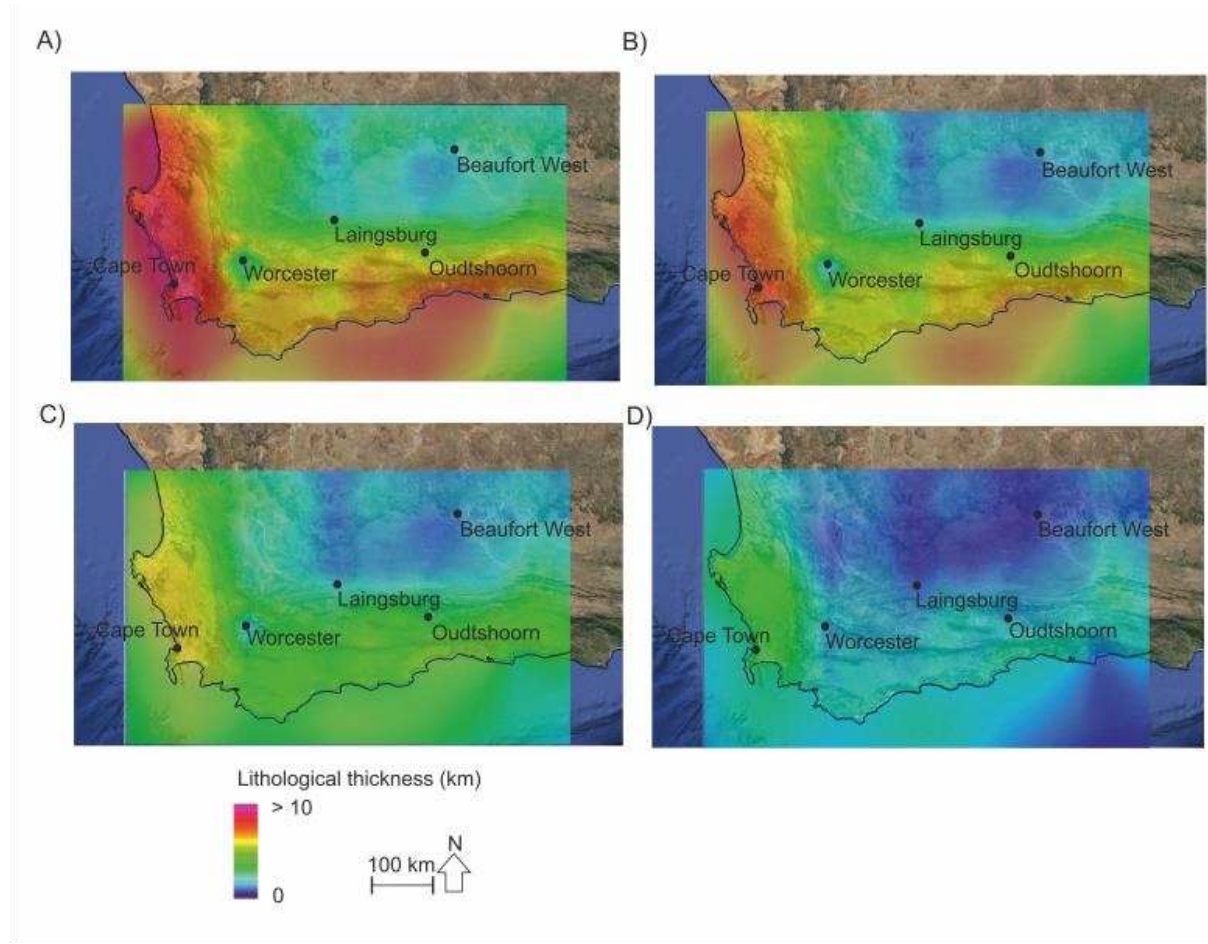
1589

1590 Figure 4 – 3D Move scenarios and example cross sections. Inset 1) a key showing  
1591 the lines used to represent present day topography and scenarios of exhumation; 2)  
1592 a location map of the 9 cross sections used in 3D Move to calculate exhumation  
1593 volumes; 3), 4) and 5) show cross sections C, F and E, respectively, which show the  
1594 maximum assumptions (with and without Drakensberg Group), median assumptions  
1595 (with and without Drakensberg Group) and minimum assumptions and; 6) shows  
1596 geological cross section F using the maximum assumptions where the top surface  
1597 represents the maximum lithological extent prior to erosion. The key for the lithology  
1598 can be found on Figure 2. Additional cross sections can be found in the online  
1599 supplementary data.



1600  
1601  
1602  
1603  
1604  
1605  
1606

1607 Figure 5 – Variation in the amount of sediment removed in southern South Africa. A)  
1608 Maximum scenario with Drakensberg lithologies present, B) maximum scenario  
1609 without Drakensberg lithologies present C) median scenario and D) minimum  
1610 scenario.



1611

1612

1613

1614

1615

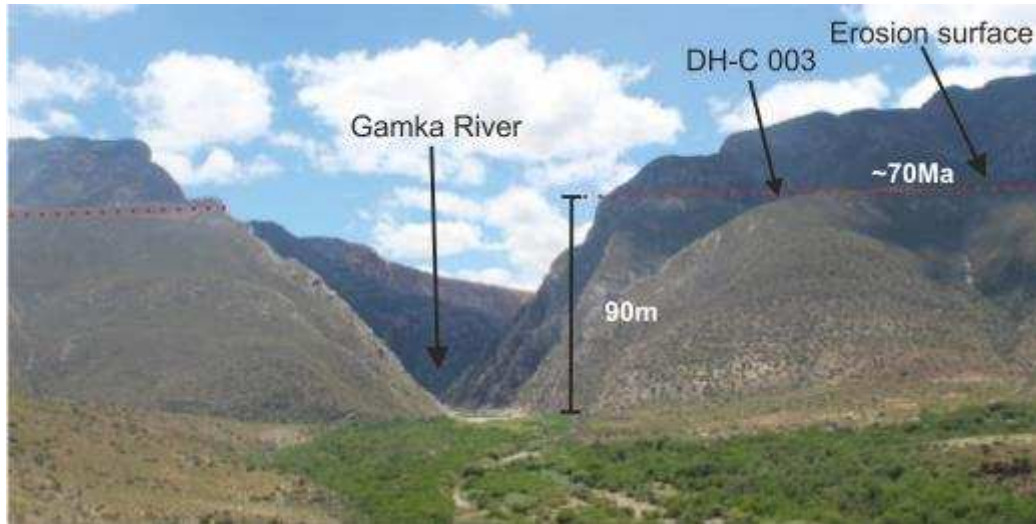
1616

1617

1618 Figure 6 – Gamkaskloof erosion surfaces and sampling point for cosmogenic dating.

1619 The transverse Gamka River dissects the Cape Fold Belt. The red dashed line

1620 represents the erosion surface sampled.



1621

1622

1623 Figure 7 – Facies descriptions and sedimentary logs from the Mesozoic basins; A)

1624 sedimentary logs from the Mesozoic Basins within the study area and; B) facies

1625 observed within the Mesozoic Basin. Inset Bi) comprises poorly-sorted to rare

1626 normally-graded clast-supported conglomerate with coarse sand to gravel grade; Bii)

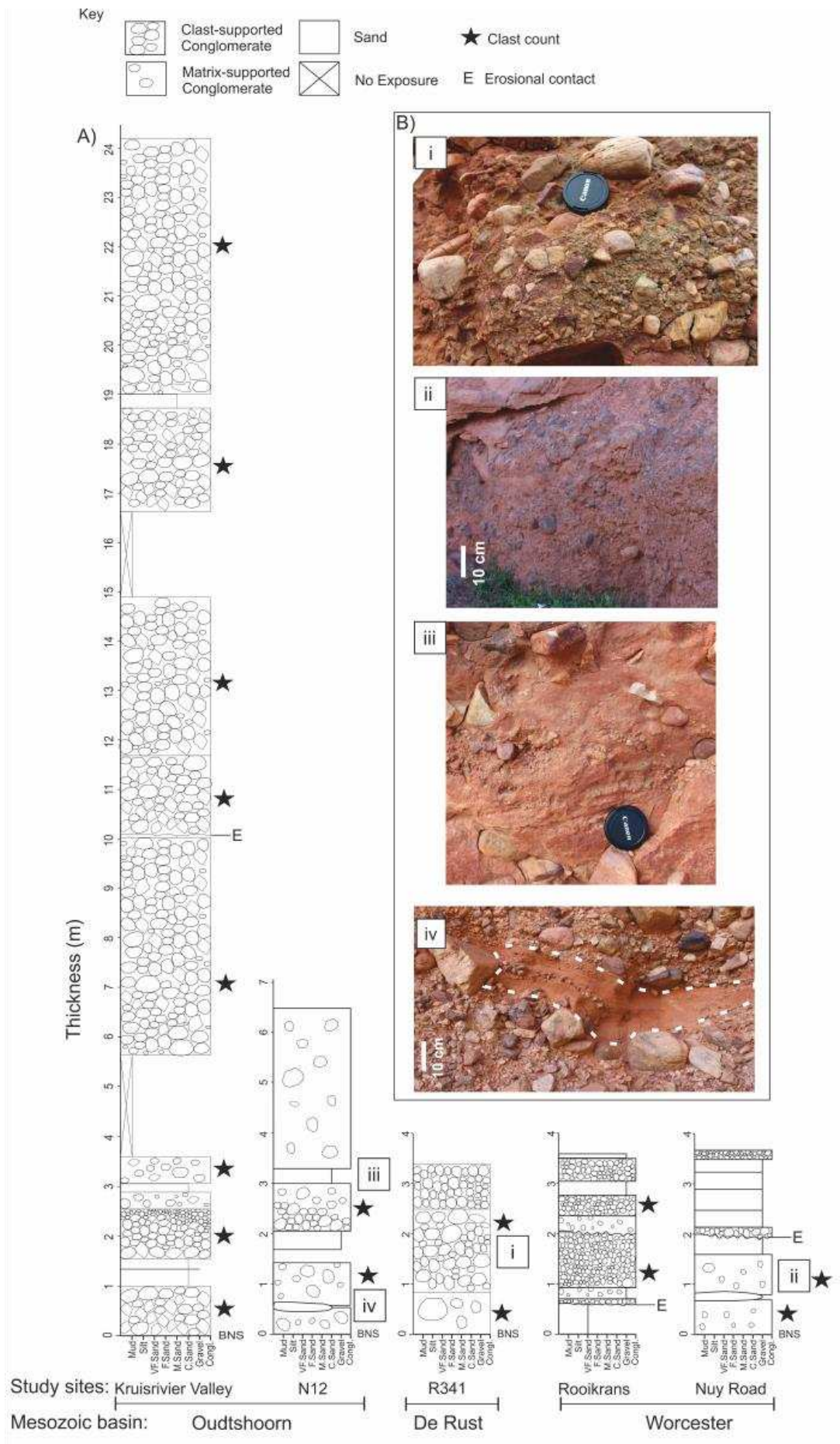
1627 comprises poorly-sorted lenticular conglomerate beds (up to 3 m) with a coarse

1628 sand matrix; Biii) structureless to weakly laminated lenticular coarse sand to gravel

1629 beds; and Biv) lenticular medium- and coarse-grained sandstones with pebble

1630 stringers (delineated by the dashed white line).

1631



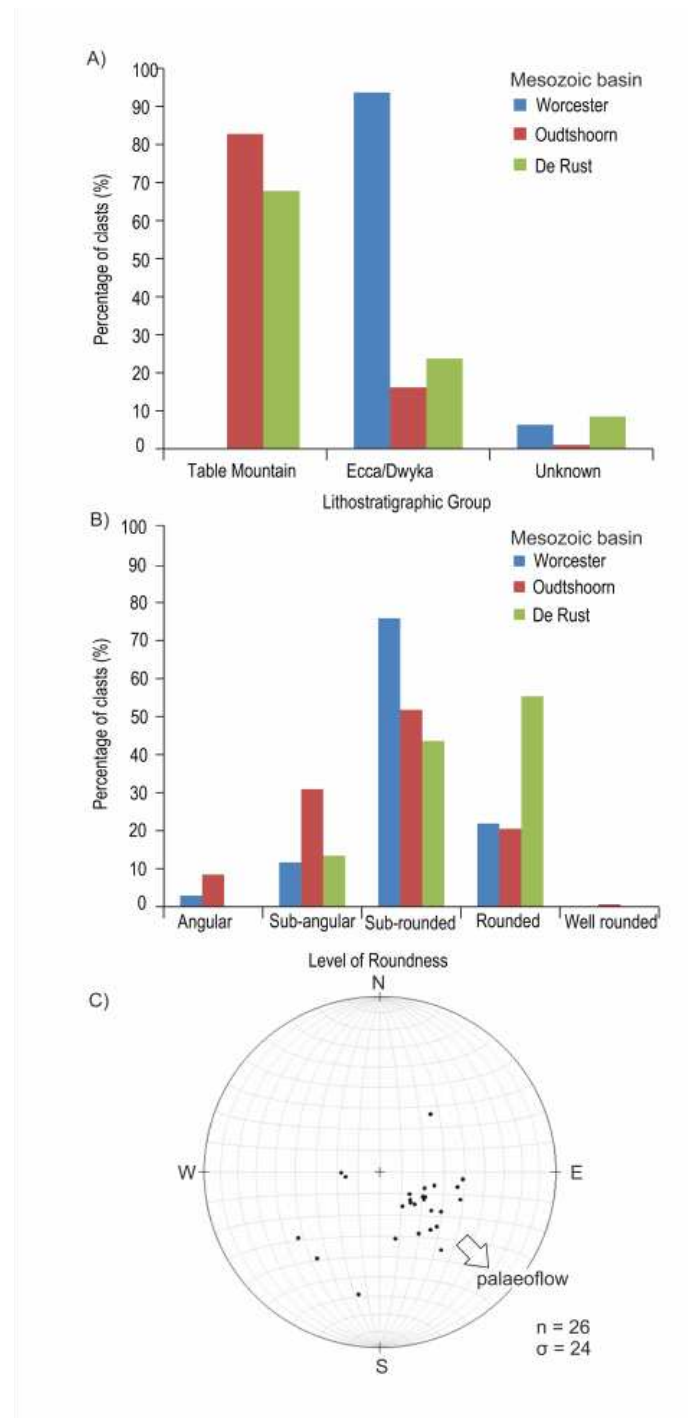
1633

1634 Figure 8 - Clast characteristics: A) clast lithology; B) clast roundness; and C)

1635 stereonet from Rooikrans study site, with poles to strike and dip of clast imbrication

1636 indicating SE palaeoflow.

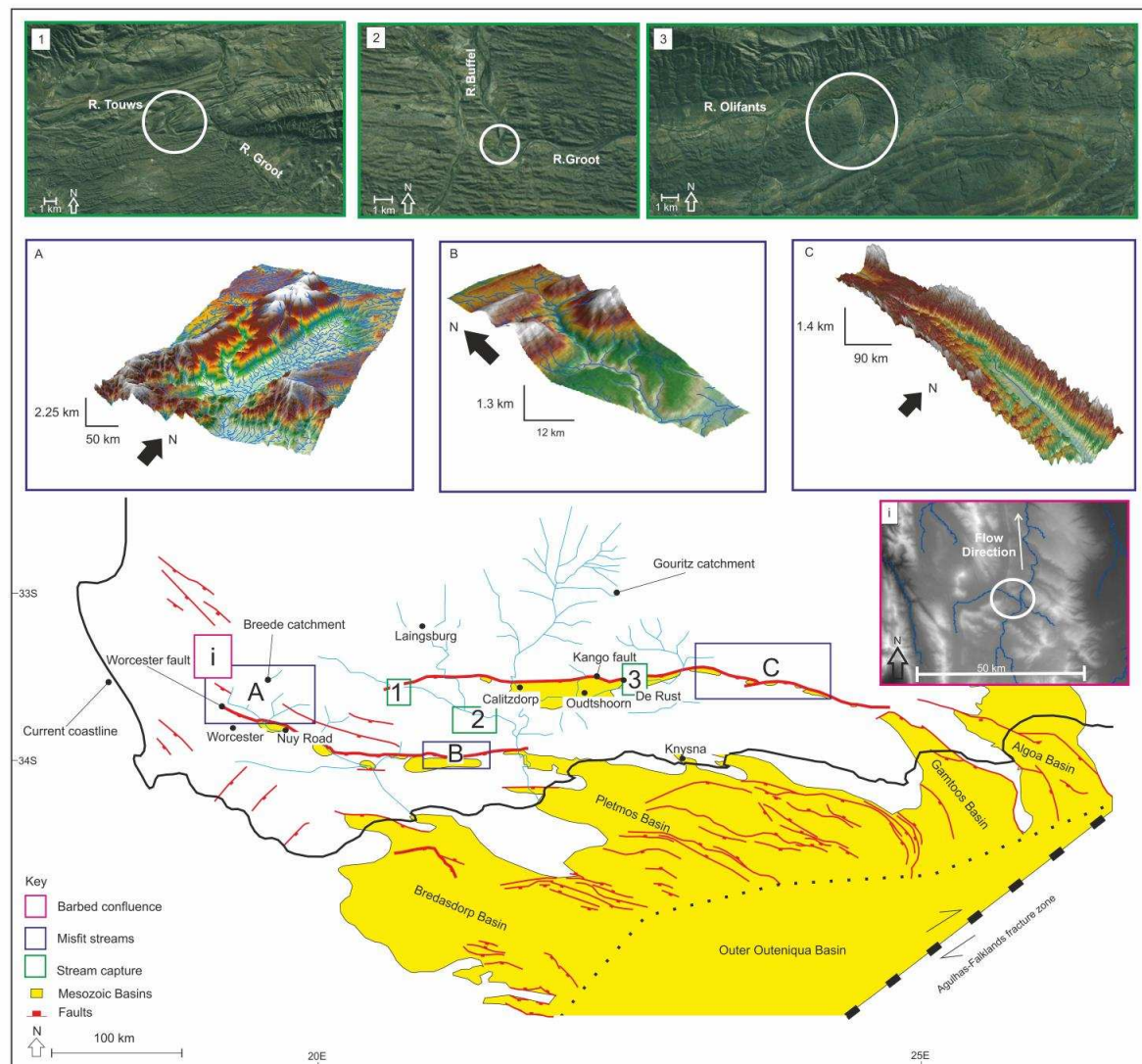
1637



1638

1639

1640 Figure 9 – Geomorphic evidence of drainage reorganisation. Main map shows the  
1641 location of inset images. (1), (2) and (3) are satellite images showing stream capture  
1642 points; (A), (B) and (C) are DEMs showing misfit streams; and (i) is a greyscale DEM  
1643 showing barbed confluences.  
1644



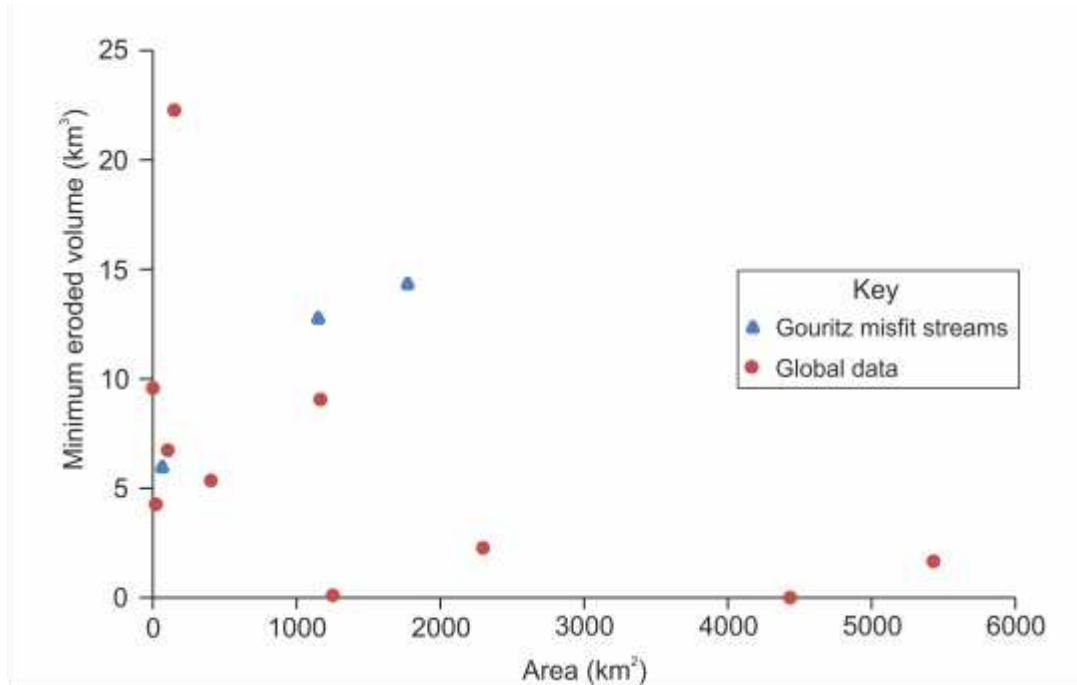
1645

1646

1647

1648

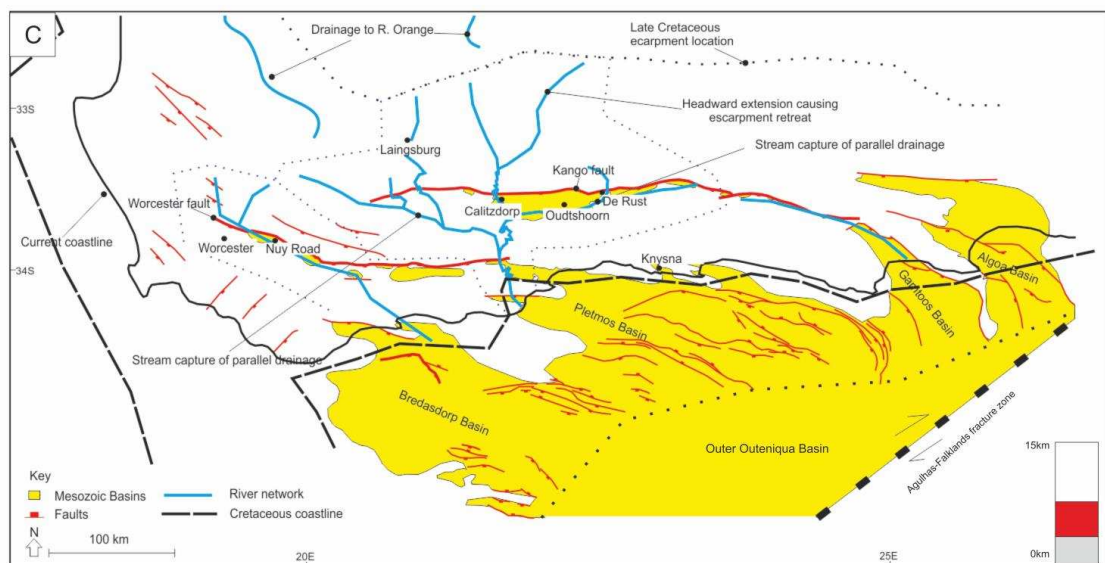
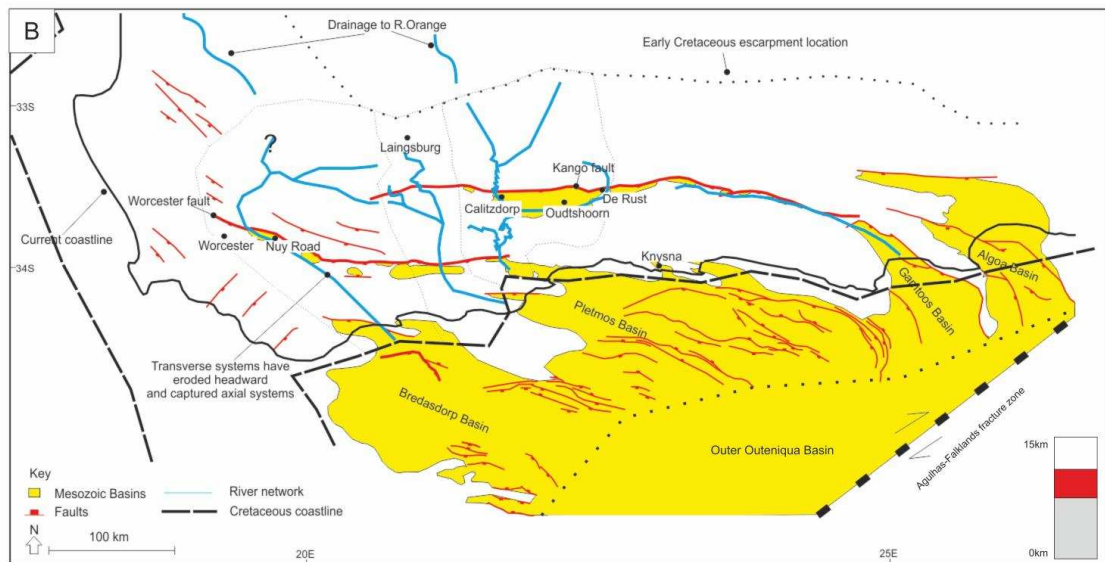
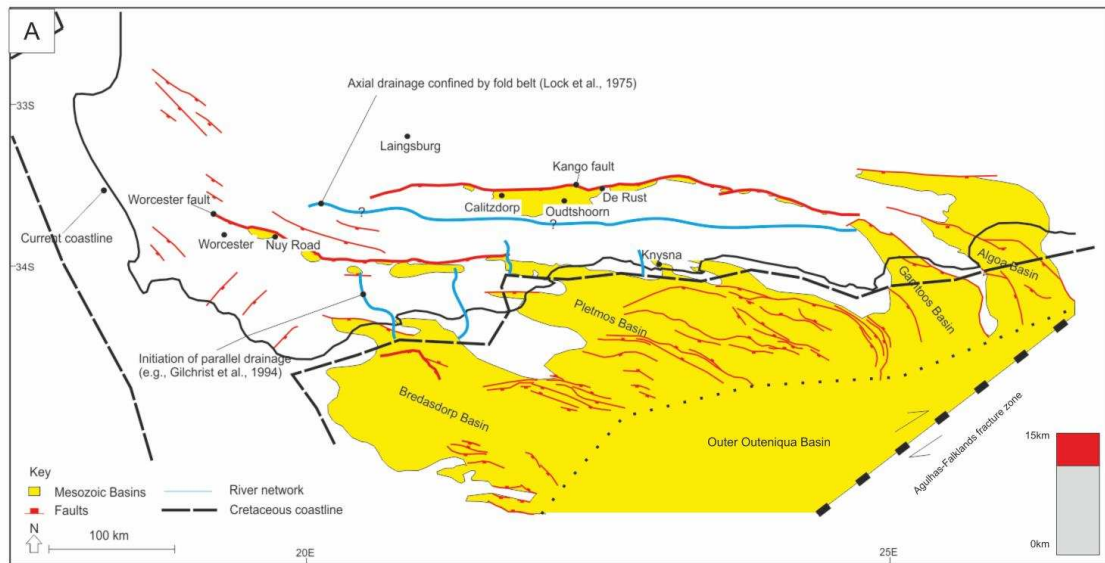
1649 Figure 10 - Comparison of how misfit the valleys in South Africa are compared to  
1650 worldwide examples. The worldwide sample data information can be found in Table  
1651 3.



1652

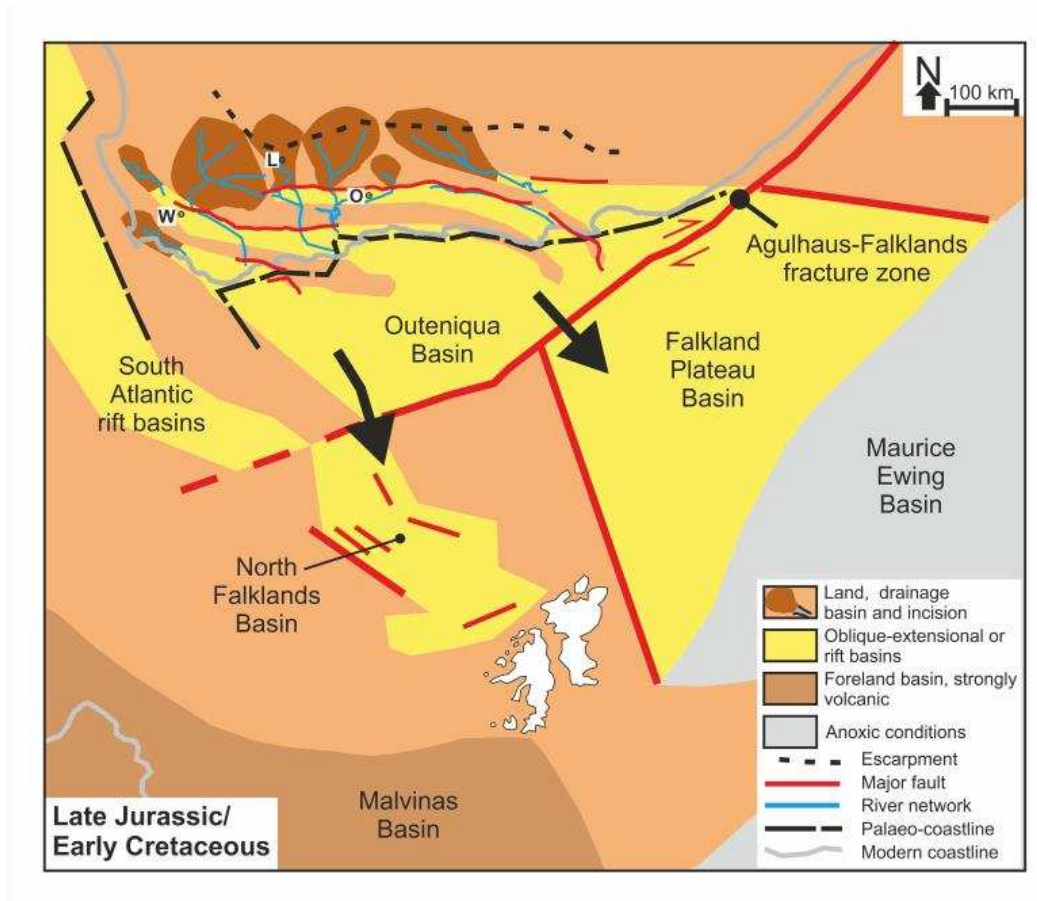
1653

1654 Figure 11 – Drainage evolution of southern South Africa from the pre-rifting of  
1655 Gondwana to the Late Cretaceous. A) Drainage just after Gondwana fragmentation  
1656 (Late Jurassic, ~150Myr); B) drainage during in Early-Mid Cretaceous (~100Myr);  
1657 and C) drainage during the Late Cretaceous (~66Myr). The inset box shows the  
1658 amount of exhumation during each time period (red) and the remaining lithological  
1659 thickness (grey) using the mean value of the scenarios in Table 7.



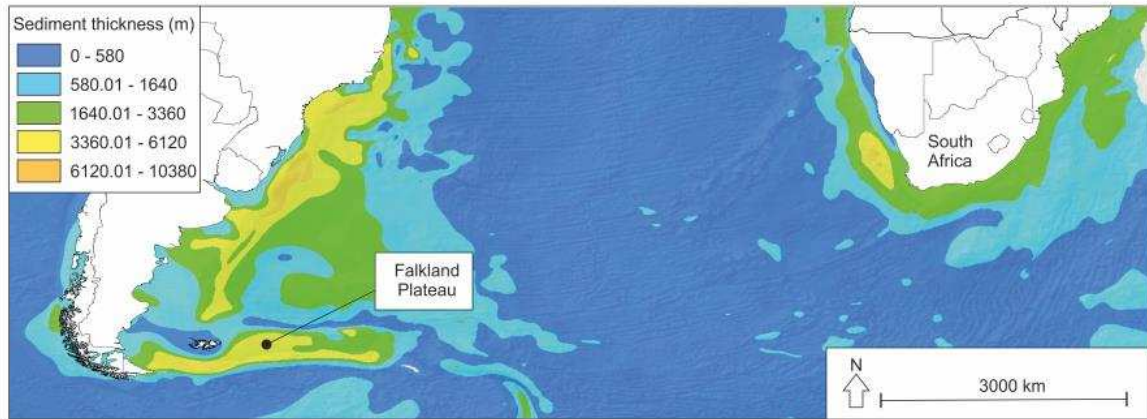
1661

1662 Figure 12 - Palaeogeographic reconstruction of the Late Jurassic to Early  
1663 Cretaceous of the southern South Atlantic region based on Macdonald et al. (2003;  
1664 their Figs. 11 and 13). Note that the Falkland Plateau Basin and the North Falkland  
1665 Basin could both have formed downstream depocentres of the Outeniqua Basin.



1666

1667 Figure 13 - Sediment thickness map for present-day southern South Atlantic from  
1668 Divins (2003) and Whittaker et al. (2013). Note the marked disparity of sediment  
1669 thickness and small land area on the Falkland Plateau. Thickness is in metres.



1670

1671

1672 Table 1 – Published data on the retreat of the Great Escarpment

Reference	Nuclides	Material	Region	Lithology	Landform	Denudation rate (m/Myr)	Integration time (Ma)
Fleming et al. 1999	<sup>36</sup> Cl	Basalt	Drakensberg (se) escarpment	Basalt	Face	50-95	0 – 1 Ma
Cockburn et al. 2000	<sup>10</sup> Be, <sup>26</sup> Al	Quartz	Central Namibian (western) margin	granite-gneiss	escarpment faces and ridges	10	
Bierman and Caffee, 2001	<sup>10</sup> Be, <sup>26</sup> Al	Quartz	Central Namibian (western) margin	granite, granite-gneiss, quartzite, pegmatite sediment	outcrop, including inselbergs	3.2	0 – 1 Ma
					escarpment highlands coastal plain	16 5 8 6.4	
Kounov et al. 2007	<sup>3</sup> He, <sup>21</sup> Ne	Quartz	Southwestern Karoo	Quartzite	Plateau surfaces	1.5-3	0 – 1 Ma
		Pyroxene	Southwestern Karoo	Dolerite	Plateau surfaces	1-2.1	
Decker et al. 2011	<sup>3</sup> He	Pyroxene	South-central Karoo and north east KwaZulu-Natal	Dolerite	Scarps, summits, plains and ridges	0.5-4	0 – 1 Ma
Brown et al. 2002	AFT, <sup>36</sup> Cl	Apatites	Drakensberg Escarpment			100-200	Cretaceous

1673

1674

1675 Table 2 – Thicknesses of key lithologies used in the geological cross sections.

1676	Group	Max Thickness	Min thickness (m)	Reference
1677		(m)		
1678	Drakensberg	1,400		Catuneanu et
1679				al., 2005
1680	Stormberg	1,400		Johnson,
1681				1976
1682	Beaufort	3,000	3,000	Adams et al
1683				2001
1684	Ecca	1,800	1,800	Adams et al.,
1685				2001
1686	Dwyka	1,300	600	Rowsell and
				De Swardt,
				1976
	Witteberg	2,000	1,700	King, 2005;
				King et al.,
				2009
	Bokkeveld	2,000	2,000	1:250,000
				Map Data
	Table Mountain	2,500	2,500	Shone and
				Booth, 2005

1687 Table 3 – Global data extracted to see how misfit the valleys of the study area are.

<b>Location</b>	<b>Latitude</b>	<b>Longitude</b>	<b>Area (km<sup>2</sup>)</b>	<b>Minimum bulk catchment erosion (km<sup>3</sup>)</b>	<b>Reference</b>
Namibian desert and escarpment	-21.304	16.217	1251.873	0.106	Bierman et al. 2007
Queensland Escarpment, Australia	-16.852	145.648	2296.749	2.269	Bierman et al. 2009
Stanley, Virginia, US	38.532	-78.603	5430.284	1.659	Duxbury 2009
Tin Can Creek, Australia	-12.453	133.270	403.6931	5.348	Heimsath et al. 2009
Peradeniya, Sri Lanka	7.261	80.595	1165.496	9.059	Hewawasam et al. 2003
Nahal Yael, Isreal	29.580	34.930	0.447029	9.576	Clapp et al. 2000
Bredbo River, Australia	-36.000	149.500	20.97207	4.269	Heimsath et al. 2006
Rio Azero, Bolvia	-19.610	-64.080	4432.853	0.003	Insel et al. 2010
Little River, Tennessee US	35.664	-83.592	149.4539	22.268	Matmon et al. 2003
Northern Flinders Range, Australia	-30.187	139.428	103.945	6.740	Quigley et al. 2007

1688

1689

1690 Table 4 – Scenarios of exhumation: recorded lithological thicknesses removed over  
 1691 key intervals

Scenario	Period 1 exhumation		Period 2 Exhumation		Period 3 exhumation		Period 4 exhumation		Period 5 exhumation		Total lithological thickness removed
	Timing	Thickness removed	Timing	Thickness removed	Timing	Thickness removed	Timing	Thickness removed	Timing	Thickness removed	
1 - Tinker et al., 2008b (using offshore accumulation rates)	136-130Ma	Equivalent to 160m onshore denudation	130 – 120 Ma	Equivalent to 190m onshore denudation	~120 – 93Ma	Equivalent to 150m onshore denudation	93 – 67 Ma	Equivalent to 270m onshore denudation	67 – 0 Ma	Equivalent to 100m onshore denudation	870m
2 - Tinker et al., 2008a (AFT)	140 – 120 Ma	1500 – 4000 m			100 – 80 Ma	2500 – 3500 m			<80 Ma	1000 m	5000 – 8500 m
3 - Wildman et al., 2015 (AFT)	Early Cretaceous	3500 – 6300 m	Mid-Late Cretaceous	3700 – 6600 m	Late Cretaceous – Early Cenozoic	1400 – 2400 m			Cenozoic	1000 m	9600 – 16300 m
4 - Wildman et al., 2016 (AFT)	Early Cretaceous	1000 – 4000 m			110 – 70 Ma	2000 – 4000 m	70 – 30 Ma	1000 – 2000 m	<30 Ma	500m	4500 – 10500 m

1692

1693

1694

1695 Table 5 – Volume of material removed from southern South Africa, data from 3D

1696 Move.

1697

Scenarios	Volume (km <sup>3</sup> )	Thickness (km)
MAXIMUM		
Extended at the coastline		
With Drakensberg	2.52 x10 <sup>6</sup>	11.30
Without Drakensberg	2.18 x10 <sup>6</sup>	9.70
To current coastline		
With Drakensberg	1.40 x10 <sup>6</sup>	6.30
Without Drakensberg	1.17 x10 <sup>6</sup>	5.30
Southerly draining catchments		
With Drakensberg	7.81 x 10 <sup>6</sup>	3.50
Without Drakensberg	6.72 x10 <sup>6</sup>	3.00
MEDIAN		
Extended at the coastline		
With Drakensberg	1.71 x10 <sup>6</sup>	7.60
Without Drakensberg	1.53 x10 <sup>6</sup>	6.80
To current coastline		
With Drakensberg	9.34 x10 <sup>5</sup>	4.20
Without Drakensberg	8.18 x10 <sup>5</sup>	3.60
Southerly draining catchments		
With Drakensberg	5.21 x10 <sup>5</sup>	2.30
Without Drakensberg	4.06 x10 <sup>5</sup>	2.10
MINIMUM		
Extended at the coastline	8.87 x10 <sup>5</sup>	4.00
To current coastline	4.67 x 10 <sup>5</sup>	2.10
Southerly draining catchments	2.60 x10 <sup>5</sup>	1.20

1698

1699

1700 Table 6 – Clast size data and standard deviation (in brackets).

Study Site	A axis (cm)	B Axis (cm)	C Axis (cm)
Worcester – Rooikrans	34 (6.99)	33 (5.05)	24 (3.73)
Worcester – Nuy Road	10 (1.72)	6 (1.19)	5 (0.95)
Oudtshoorn – Kruisrivier	39 (6.19)	29 (4.11)	18 (2.96)
Oudtshoorn – N12	22 (5.34)	10 (3.11)	10 (2.28)
De Rust	52 (9.55)	33 (6.83)	28 (5.04)

1701

1702

1703 Table 7 – Exhumation scenarios: variation in the amount of exhumed material based  
 1704 on scenarios within Table 4 applied to data from 3D Move (Table 5). The main  
 1705 number is the maximum exhumation and the number in brackets relates to the  
 1706 median exhumation.  
 1707

	Scenario 1 – Tinker et al., 2008b		Scenario 2 – Tinker et al., 2008a		Scenario 3 – Wildman et al., 2015	
	Maximum	Maximum – southern draining	Maximum	Maximum – southern draining	Maximum	Maximum – southern draining
Late Jurassic - Early Cretaceous (~140-~120Ma)	18.39%		30 .00 – 47.06%		36.46 – 38.65%	
Early - Mid Cretaceous (~130-120Ma)	21.84%		3.39 – 5.31 km (2.28 – 3.58km)	1.05 – 1.65km (0.69 – 1.08km)	4.11 – 4.37km (2.77 – 2.94km)	1.28 – 1.35km (0.84 – 0.88km)
Late Cretaceous (~120-~70Ma)	17.24%		41.18 – 50%		38.54 – 40.49%	
Late Cretaceous – Early Cenozoic (~90-~70Ma)	31.03%		1.94km (1.31km)	0.60km (0.40km)	4.35 – 4.57km (2.93 – 3.08km)	1.35 – 1.42km (0.89 – 0.93km)
Early Cenozoic to Late Cenozoic (~80Ma to 0Ma)	1.50%		11.76 – 20%		14.58 – 14.73%	
	1.30km (0.87km)	0.40km (0.26km)	1.33 – 2.26km (0.89 – 1.52km)	0.41 – 0.70 km (0.27 – 0.46km)	0.69 – 1.18 km (0.46 – 0.79km)	0.71 – 1.21km (0.14 – 0.24km)